

The Role of Crystallography and Nanostructures on Friction in FCC Metals

S . V. Prasad, J. R. Michael, C. C. Battaile, P. G. Kotula

Sandia National Laboratories, Albuquerque, NM

svprasa@sandia.gov

B. S. Majumdar

New Mexico Institute of Mining & Technology, Socorro, NM

MS&T'11

Materials Science & Technology

October 16-20, 2011 Columbus, OHIO

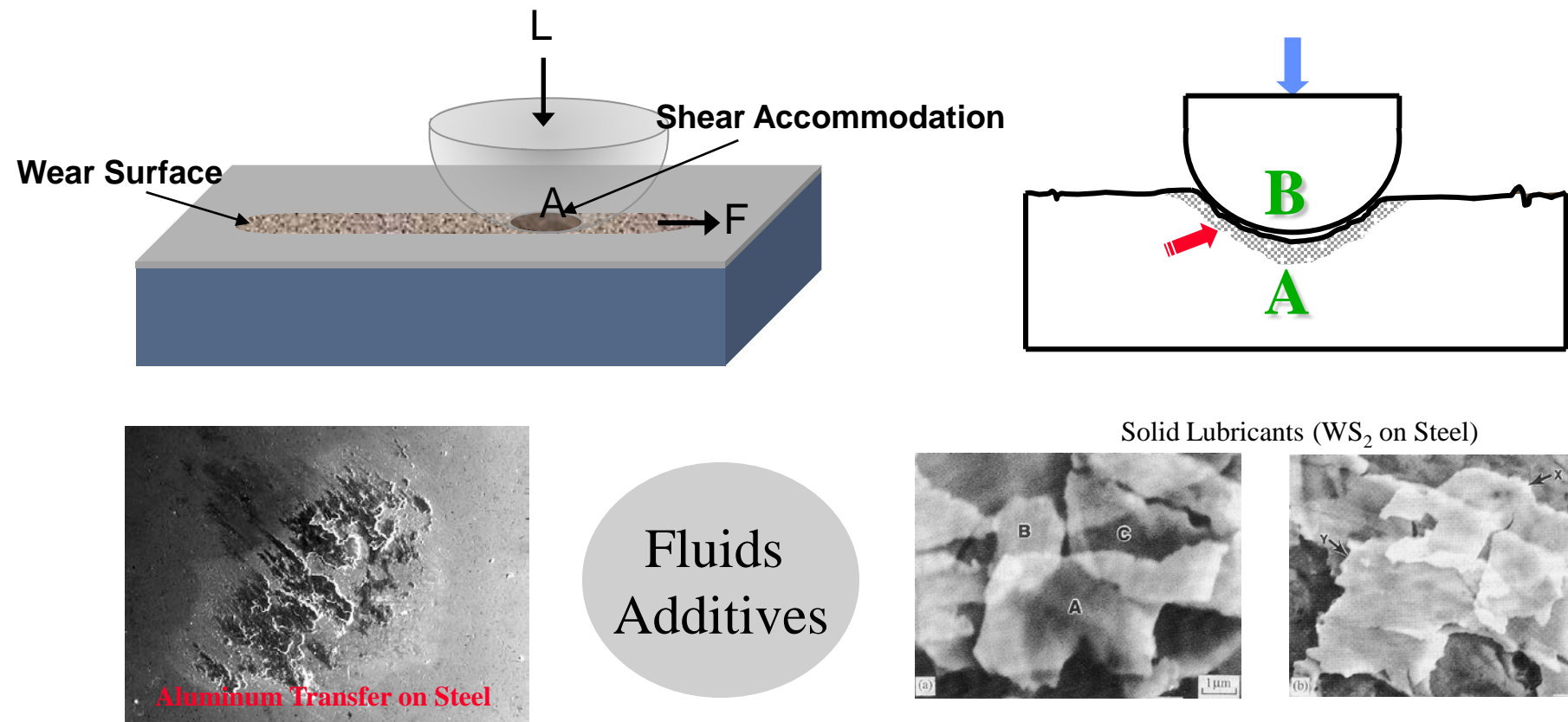


Sandia National Laboratories is a multi-program laboratory managed and operated by Sandia Corporation, a wholly owned subsidiary of Lockheed Martin Corporation, for the U.S. Department of Energy's National Nuclear Security Administration under contract DE-AC04-94AL85000





Tribology is a Systems Property

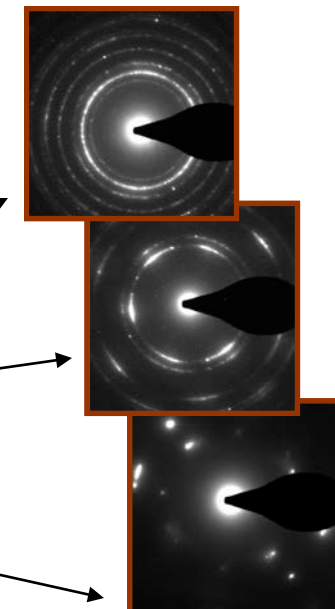
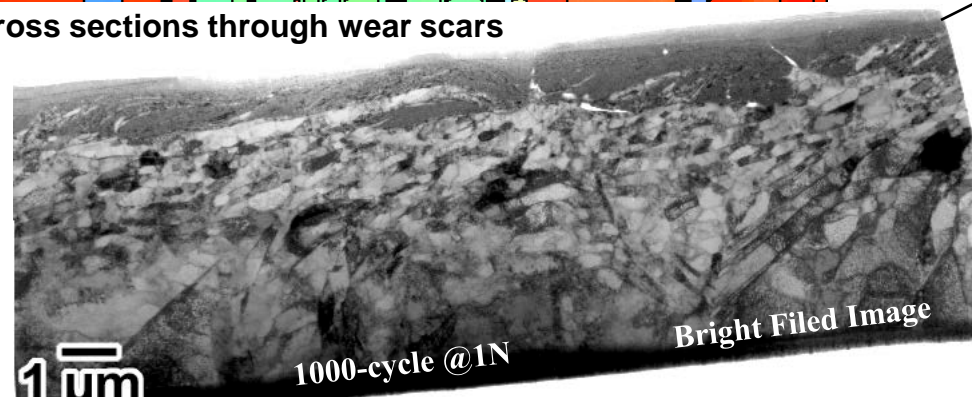
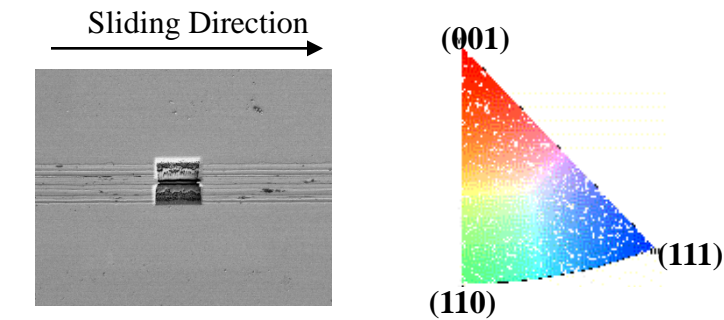
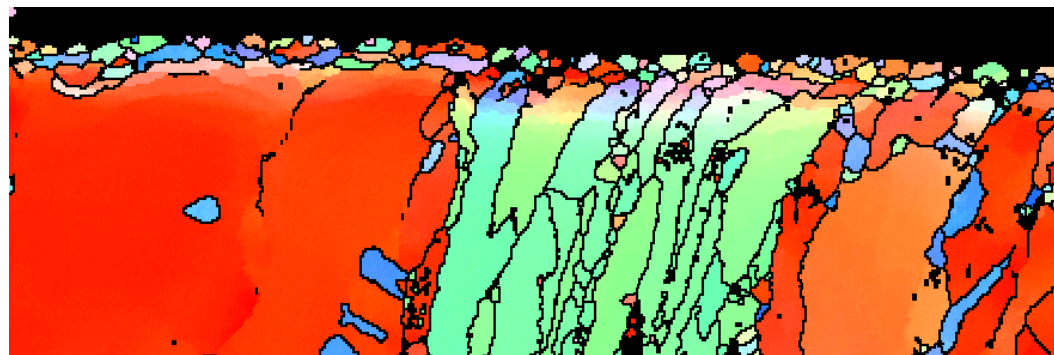
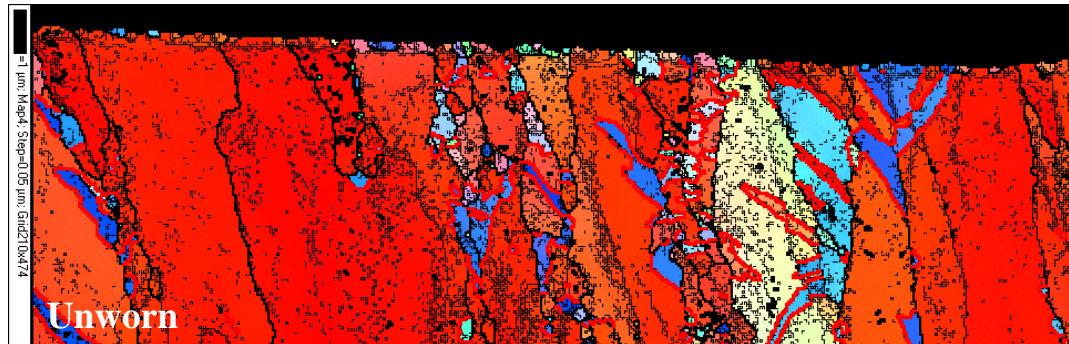


Major Theme

Fundamental Understanding of the Evolution of
Friction-induced grain structure in single crystals metals
(Start from the Clean Slate)

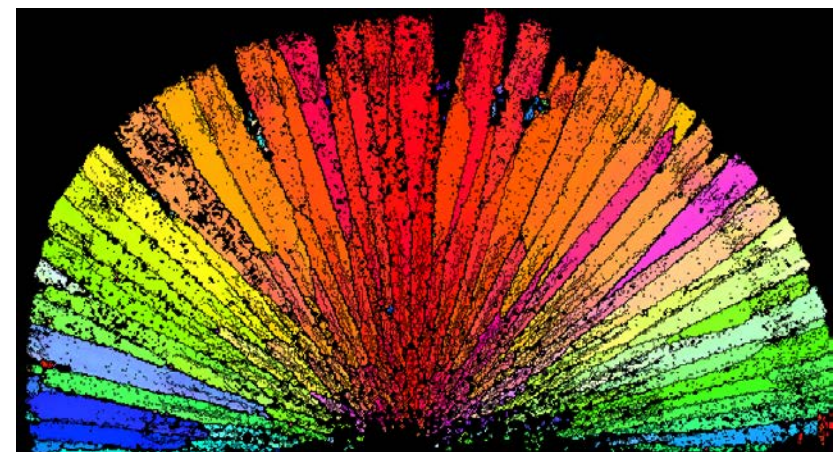
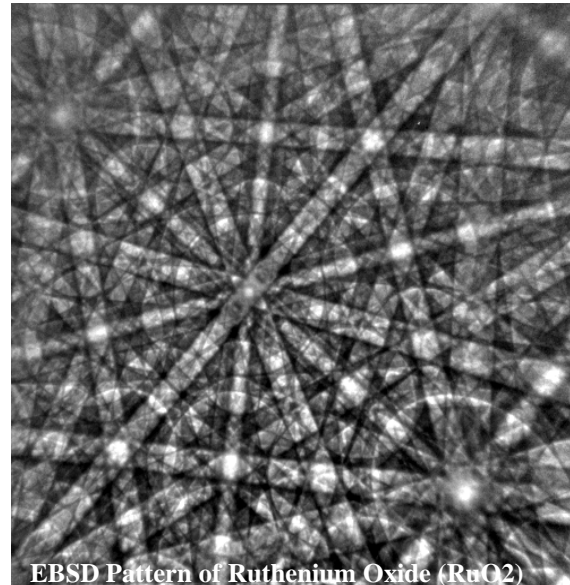
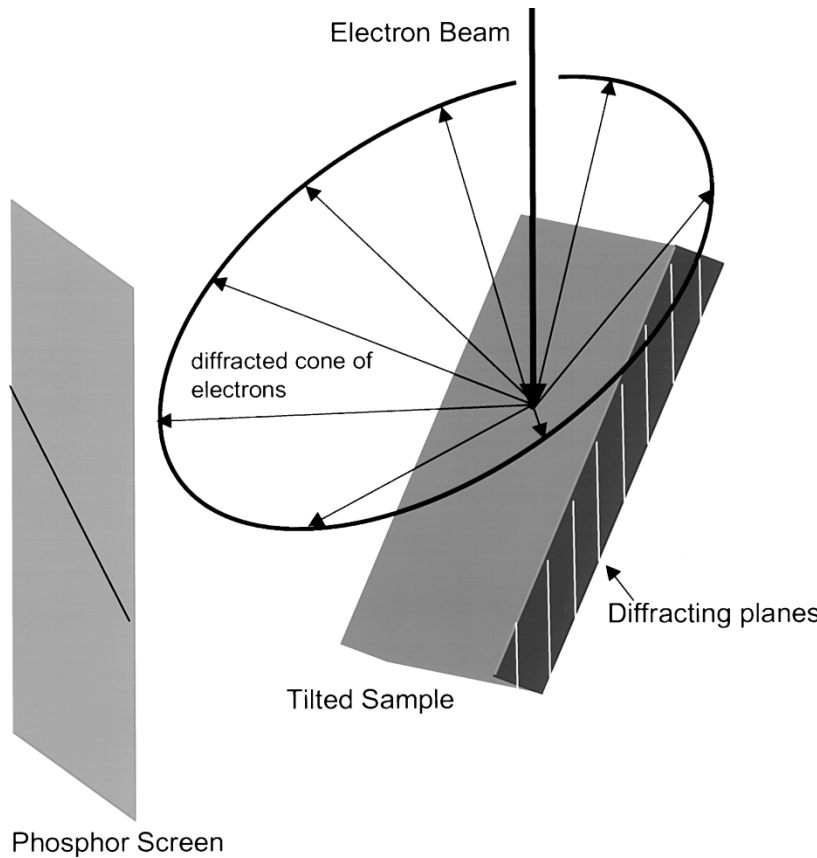


Modern Tools: FIB, Orientation Imaging, TEM

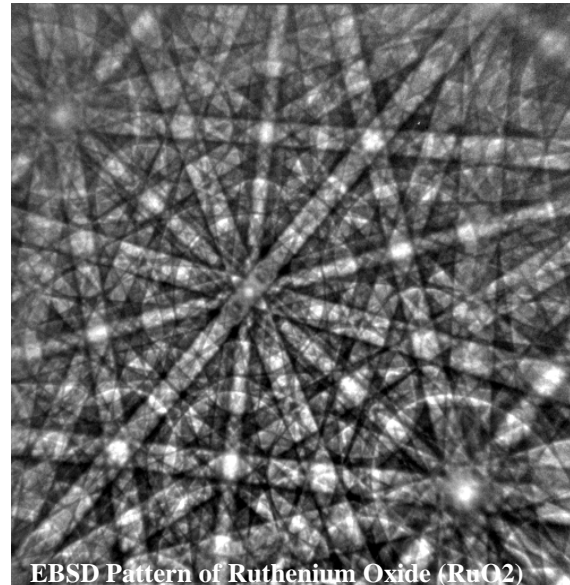
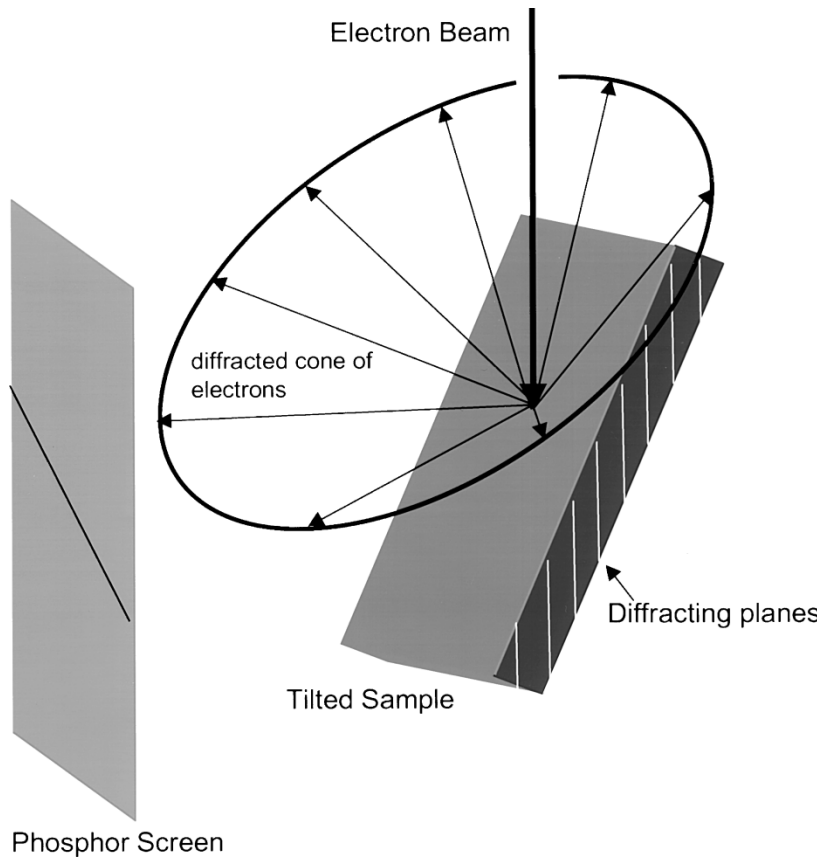


Prasad SV, Michael JR, Christen TR, *Scripta Materialia* 48 (2003) 255

Electron Backscatter Diffraction (EBSD) in the SEM



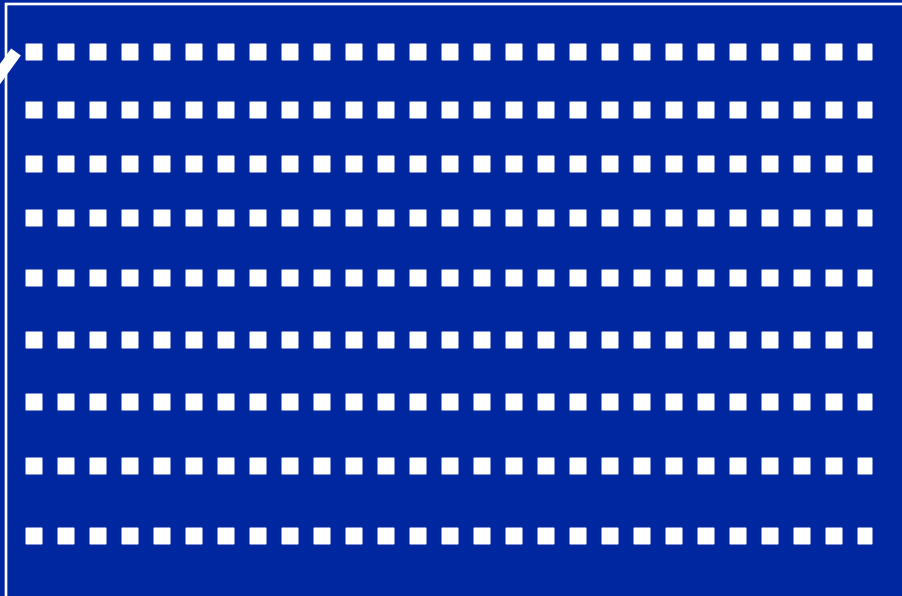
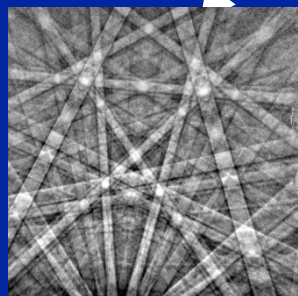
Electron Backscatter Diffraction (EBSD) in the SEM



ZnO Rods



Automated EBSD Pattern Indexing



SEM image with pixels for EBSD

**Step size dictated by microstructure
and level of detail needed.**

Minimum step size < 20nm!

1. Scan area of interest pixel by pixel.
2. Collect EBSD pattern
3. Located 4 – 7 lines on pattern – Hough transform
4. Calculate angles between bands
5. Compare with known unit cells (short list)
6. Index pattern
7. Calculate orientation
8. Move to next pixel

Modern systems can do this up to 50 times per second!

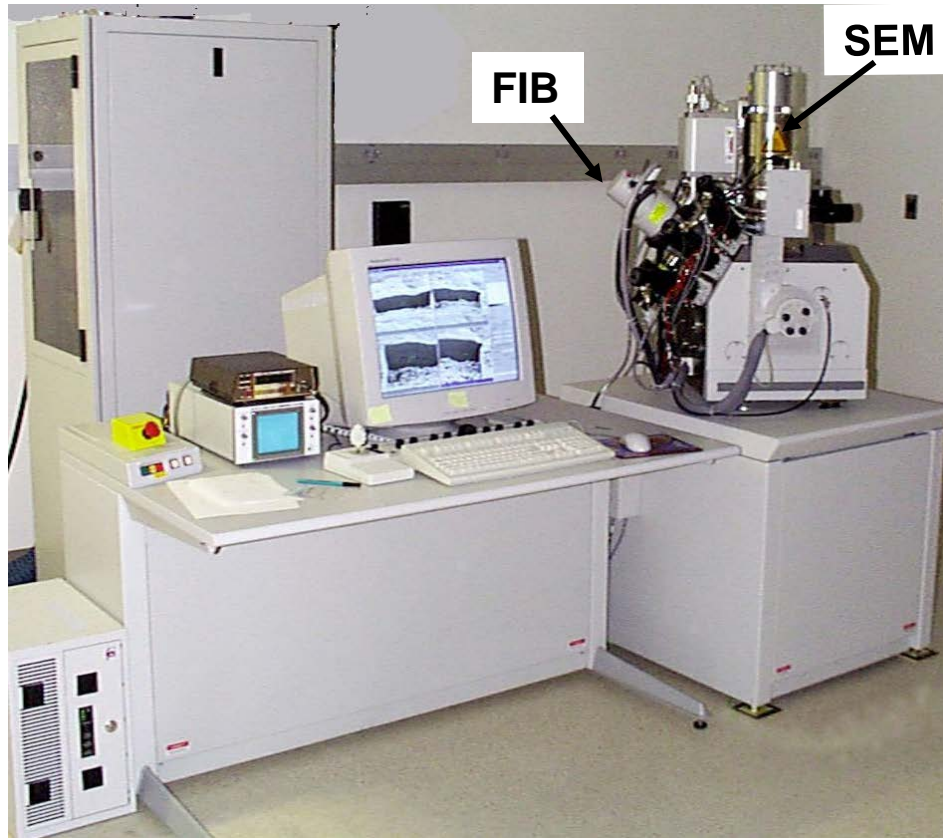


Typical FIB Configurations

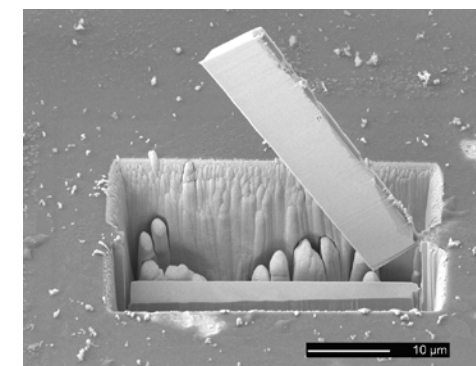
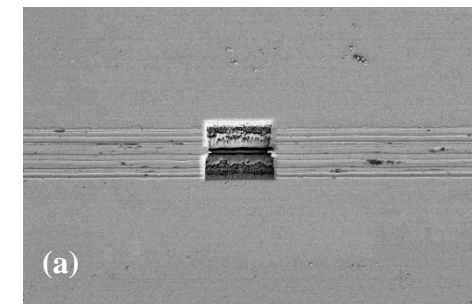
Conventional Techniques

- Ion Milling (Dimpling)
- Electropolishing
- Ultramicrotomy


(-) (-) (-)
Not site specific



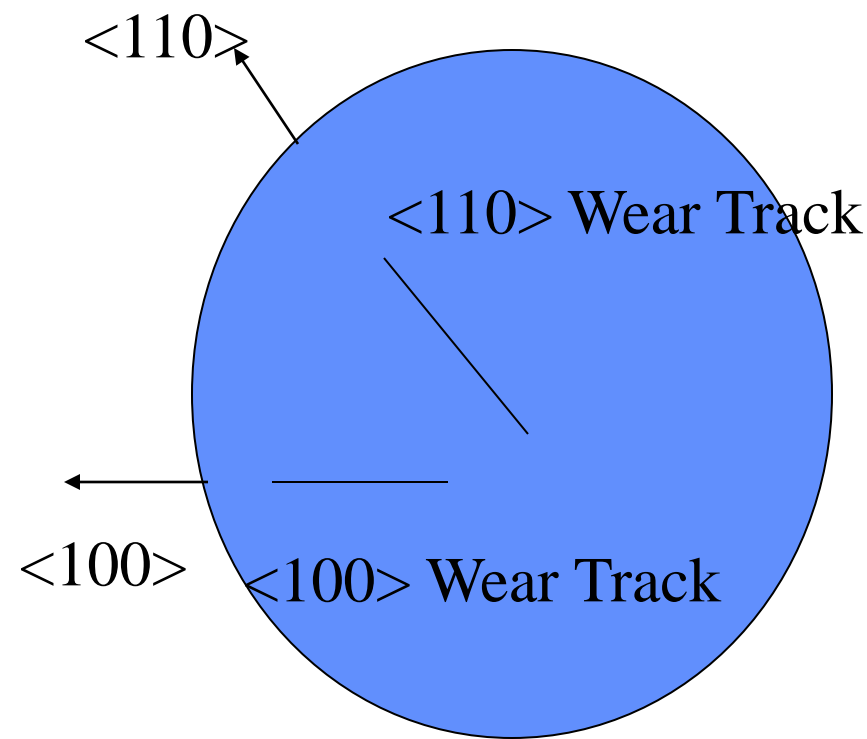
Sliding Direction



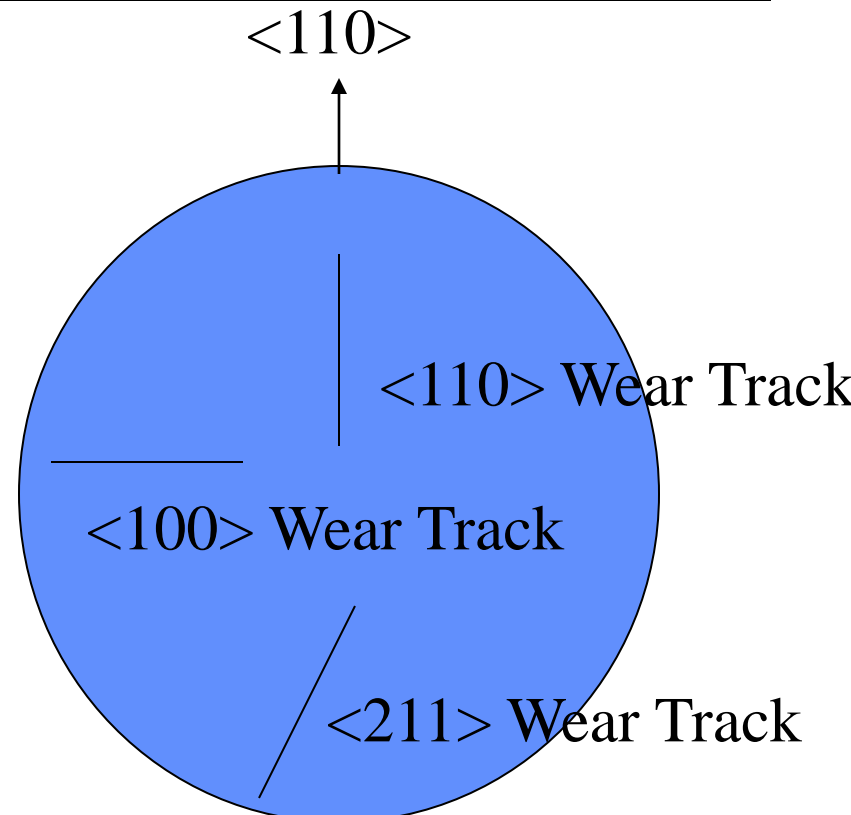
Dual-beam system from FEI: Both a FIB column and a SEM column are present on one sample chamber.



Crystallographic configurations for friction testing on single crystal Ni

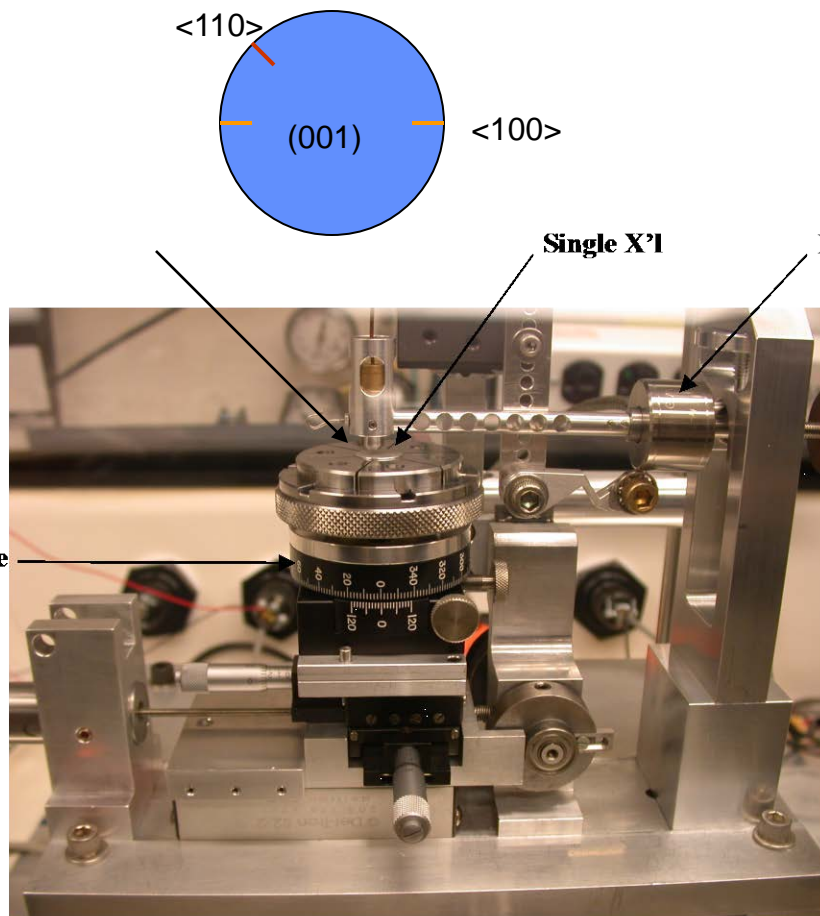


(001) Crystal Face

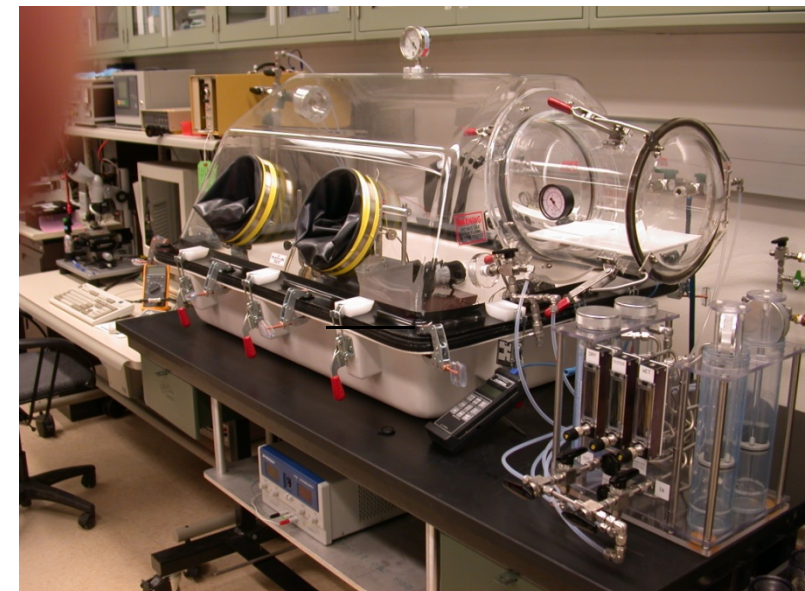


(011) Crystal Face

Rotary Friction Test Module



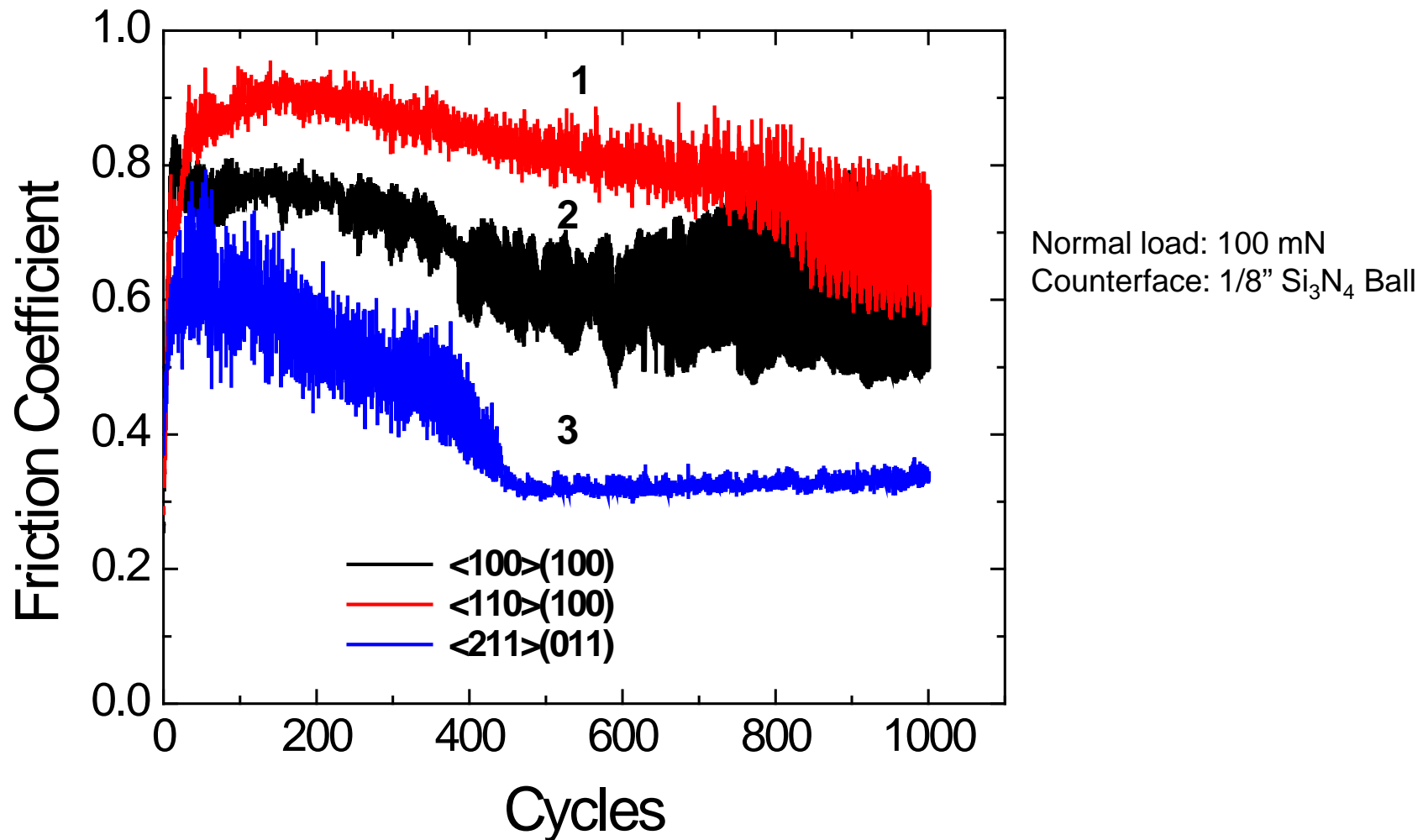
Rotary Stage for Single Crystal Alignment



Environmental chamber

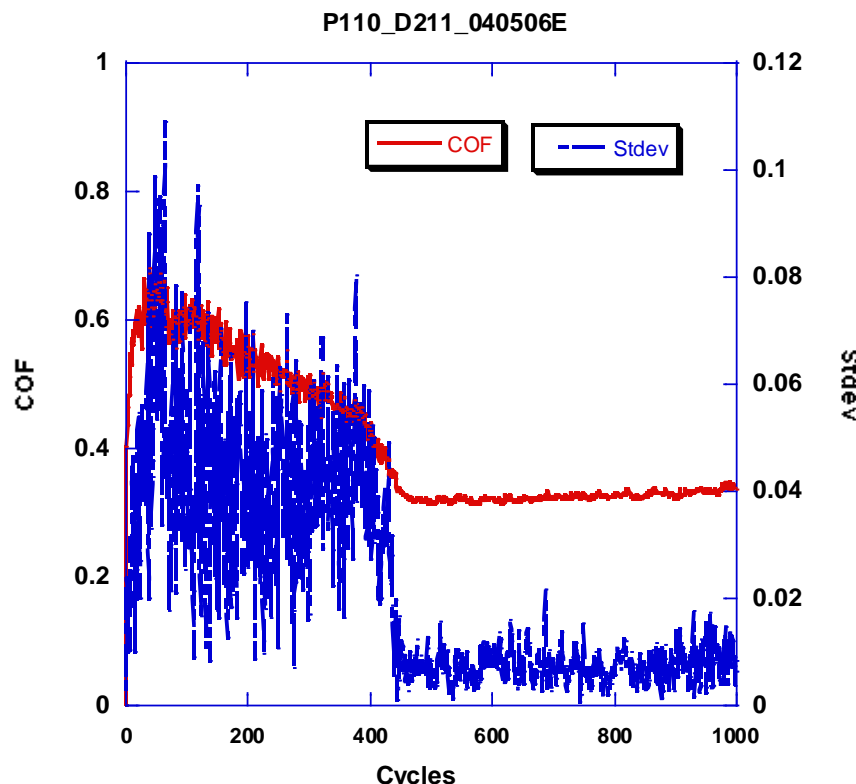
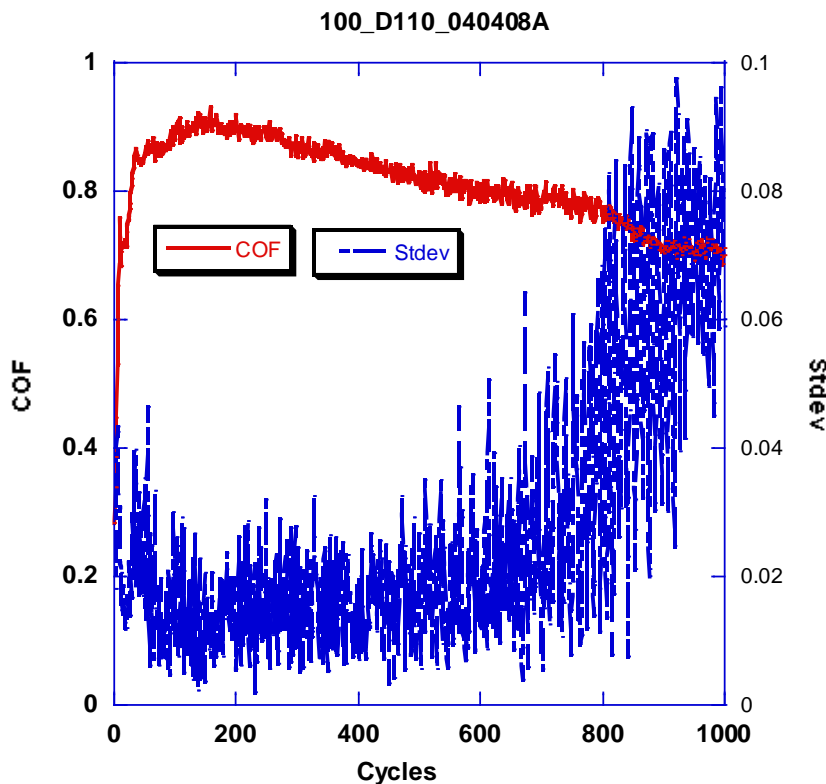


Friction is dependent on crystallographic orientations



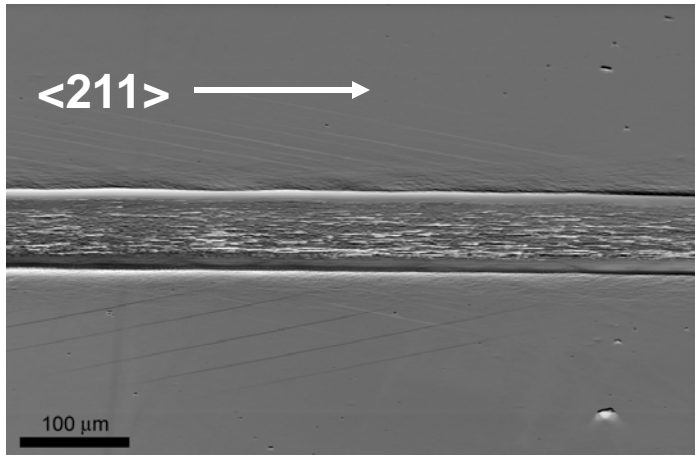


Friction data on two crystallographic directions

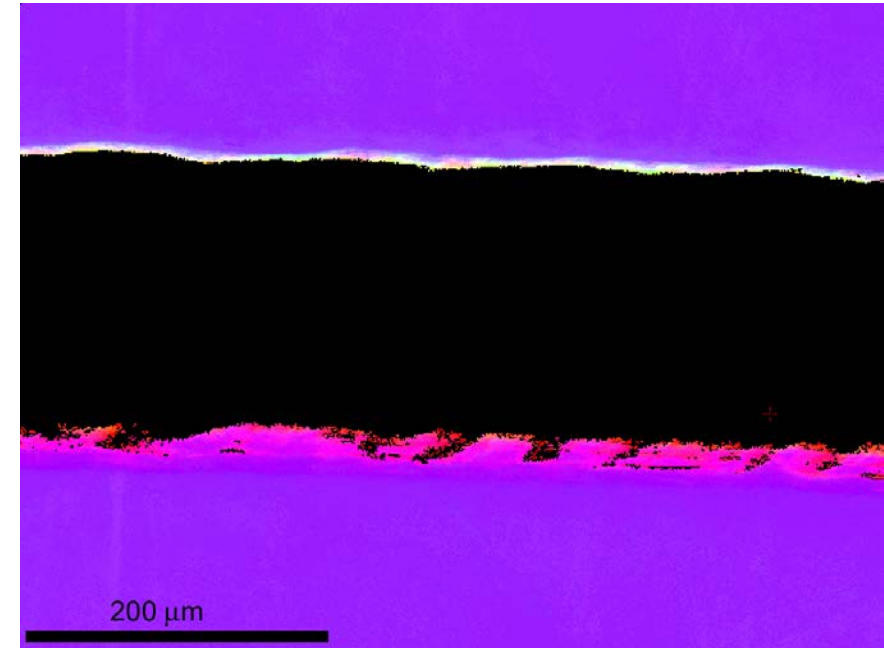
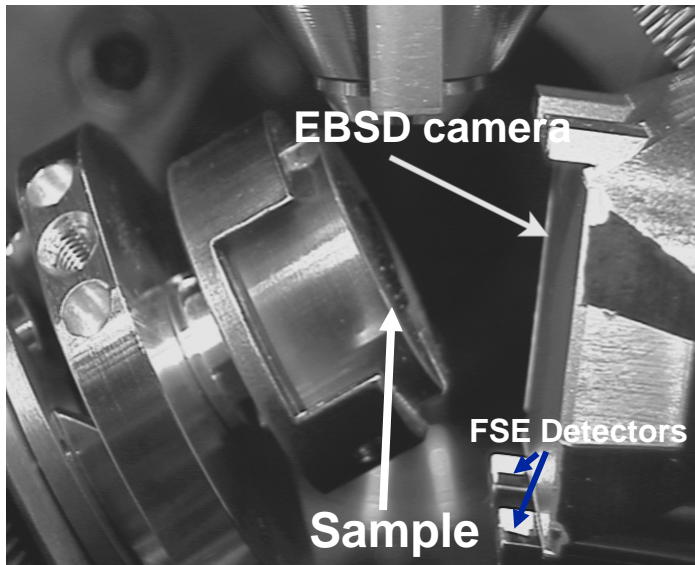




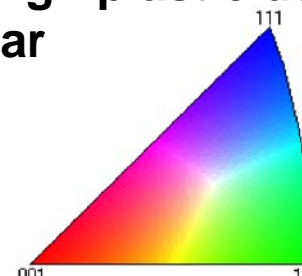
SEM imaging (FSE) and EBSD of wear scars in plan-view



SEM image of forward scattered electrons (FSE). Note visibility of $\{111\}$ slip traces. (Image not corrected for 70° tilt.)



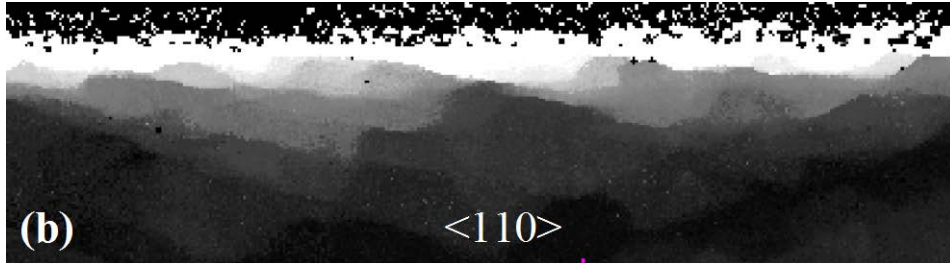
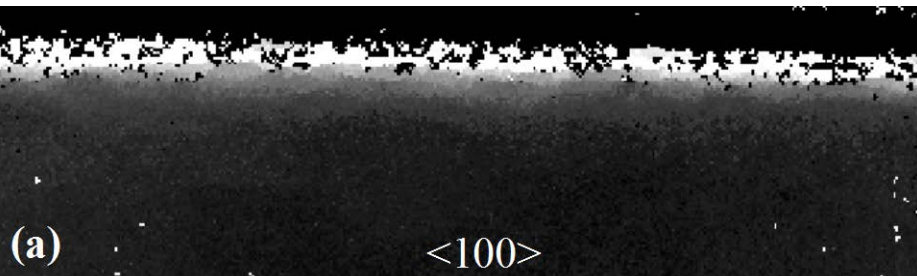
EBSD IPF map with respect to the sliding direction. Note dark region due to high plastic deformation in wear scar



Larger tilts produce higher quality EBSD patterns

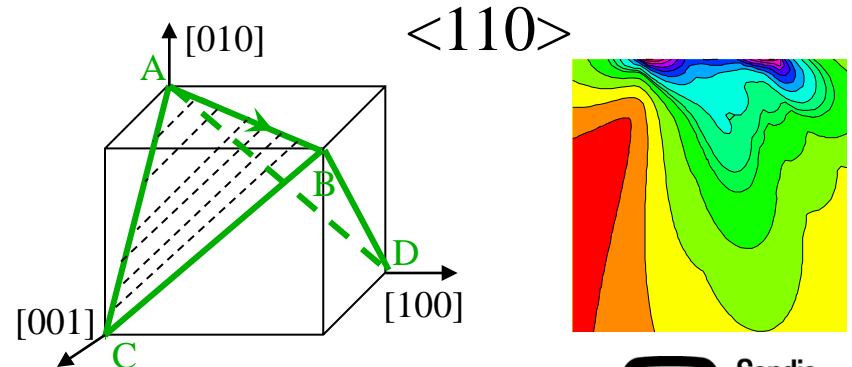
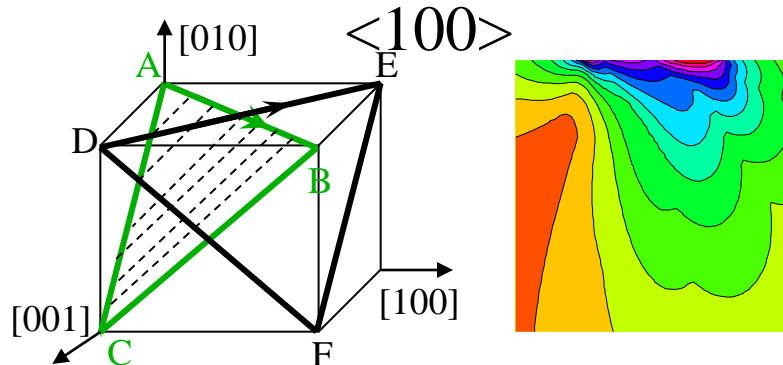


Depth of deformation is related to crystallography

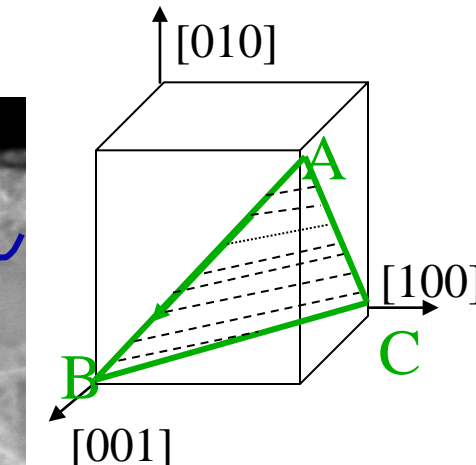
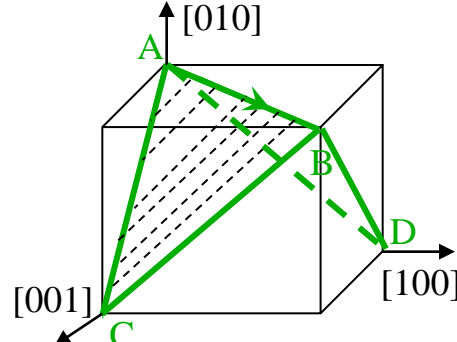
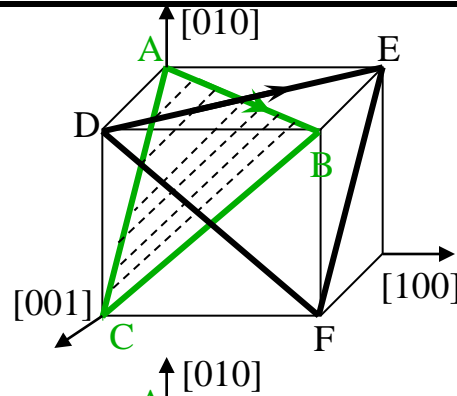
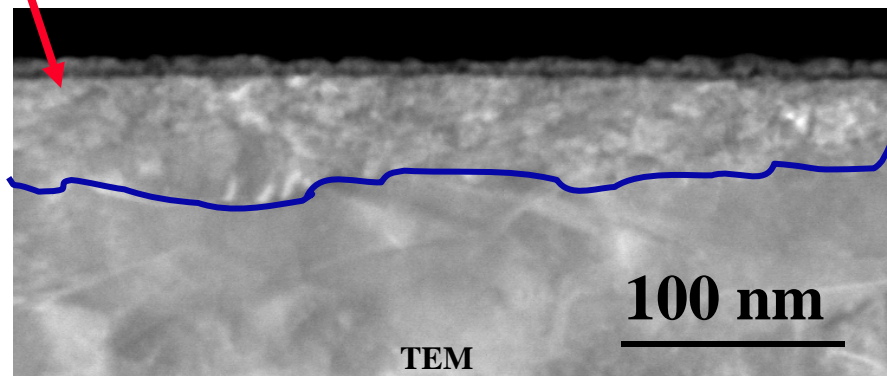
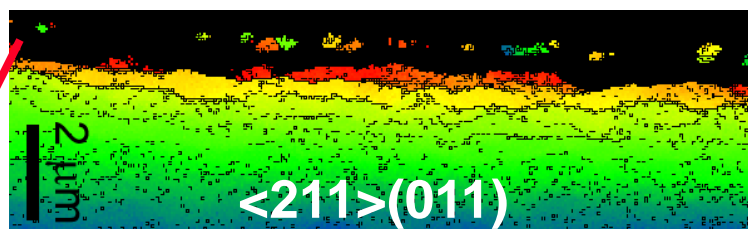
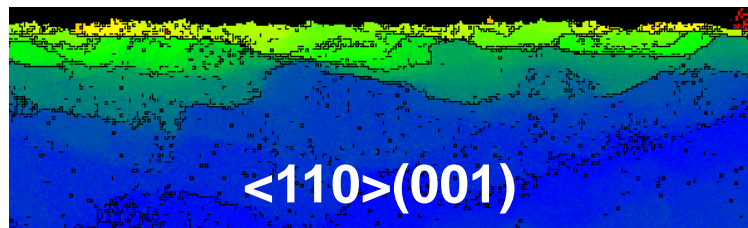
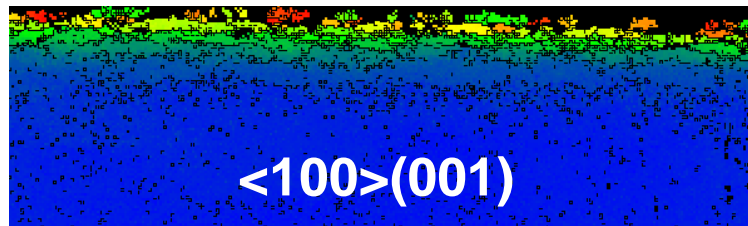


Maps showing the orientation changes relative to undeformed regions on (100) crystal surface. Brighter color represents larger orientation change. The magnitude of orientation change was about 6° total in for the friction track in the $<100>$ direction and about 13° for the track in $<110>$ direction.

Slip system orientations show intersecting slip systems for $<100>$ wear (ABC plane in AB direction, and DEF in DE), but not for $<110>$ (ABC in AB and ABD in AB), suggesting more hardening for $<100>$. Color maps of resolved shear stress from analyses of plastic deformation show the strong asymmetry induced by sliding (as opposed to static) contact.



Depth of deformation is related to crystallography



Strong dislocation interactions- high work hardening

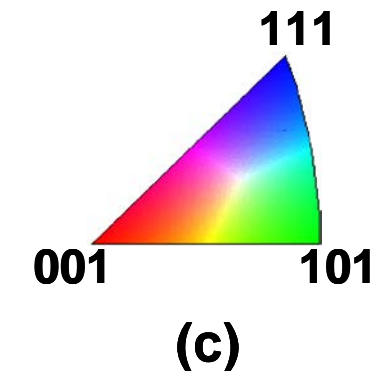
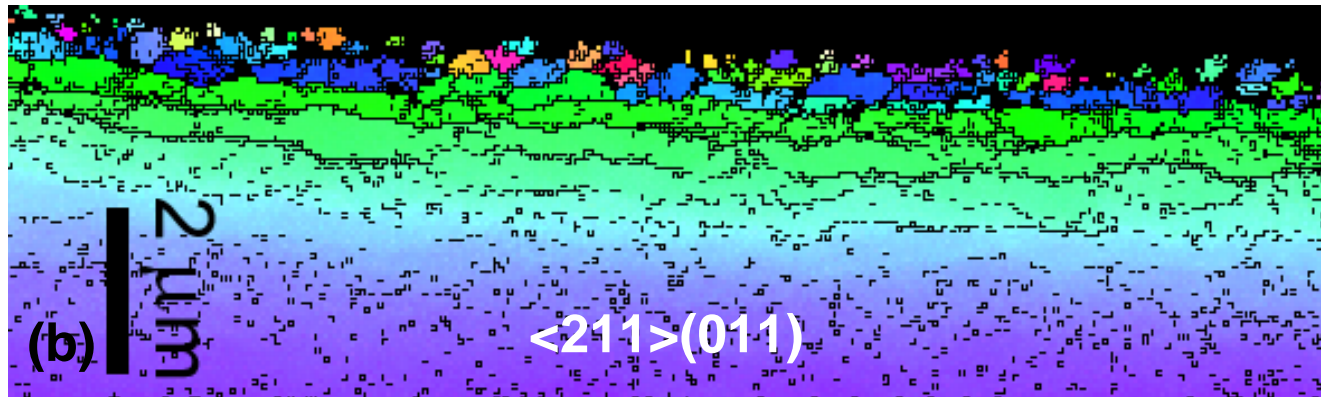
Weak dislocation interactions- low work hardening

Very weak dislocation interactions- low work hardening – rapid recrystallization

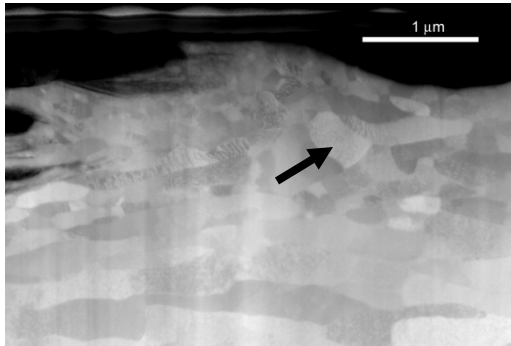


EBSD: Crystallographic maps

(a)

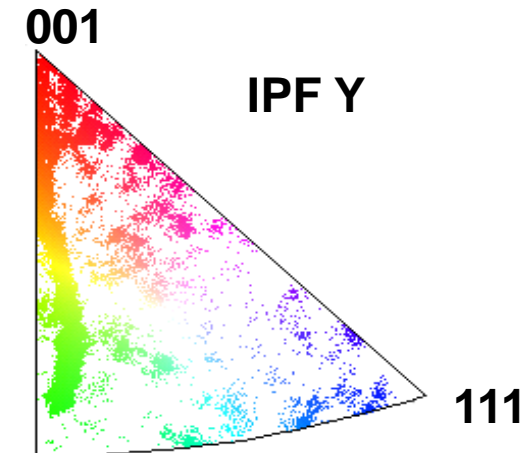
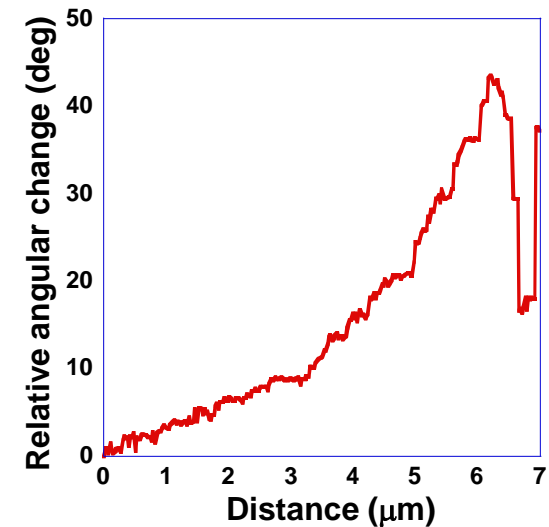
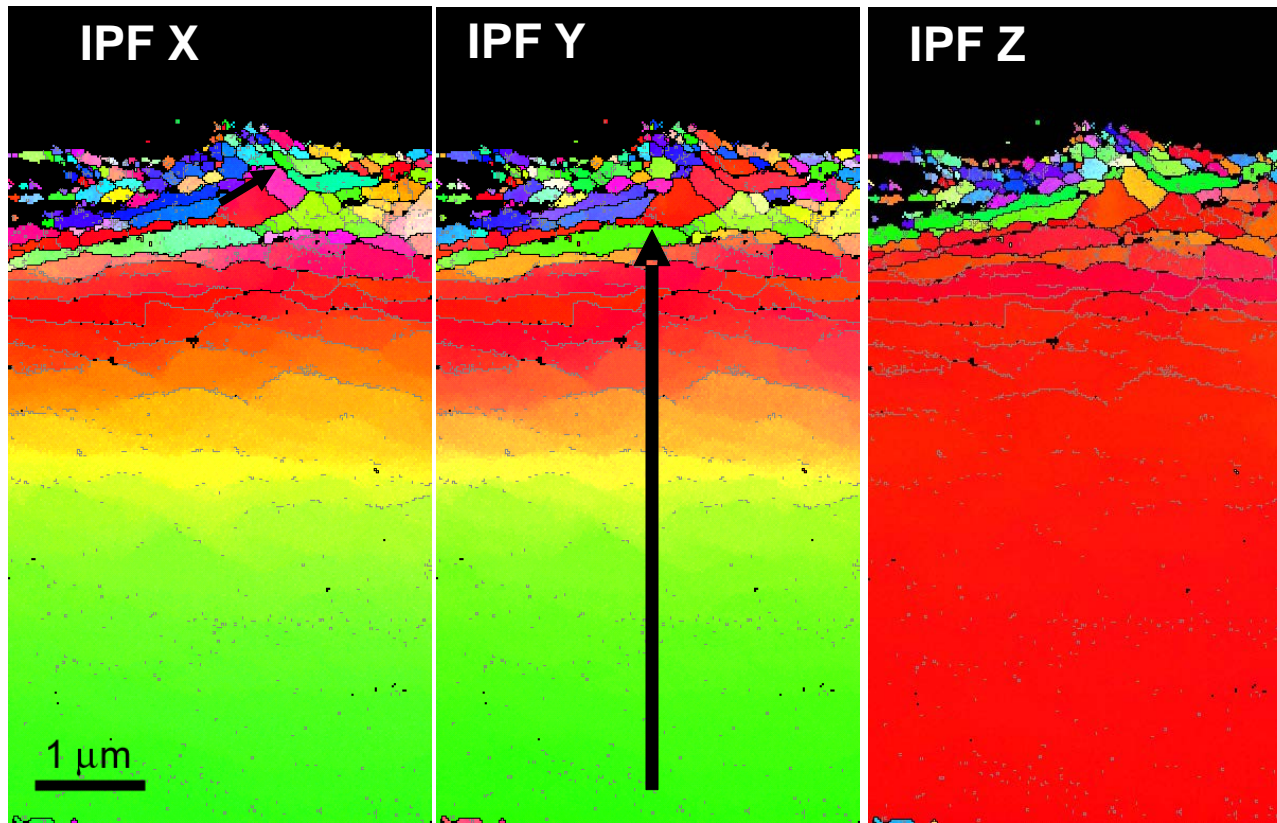
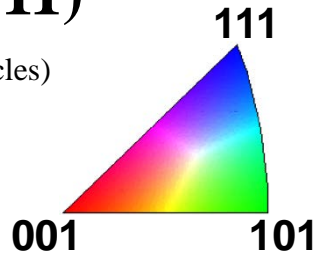


Relationship between crystallography and sliding-induced deformation



$<110>$ on (011)

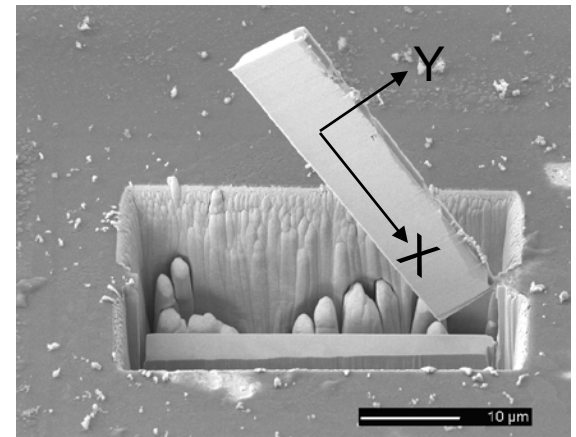
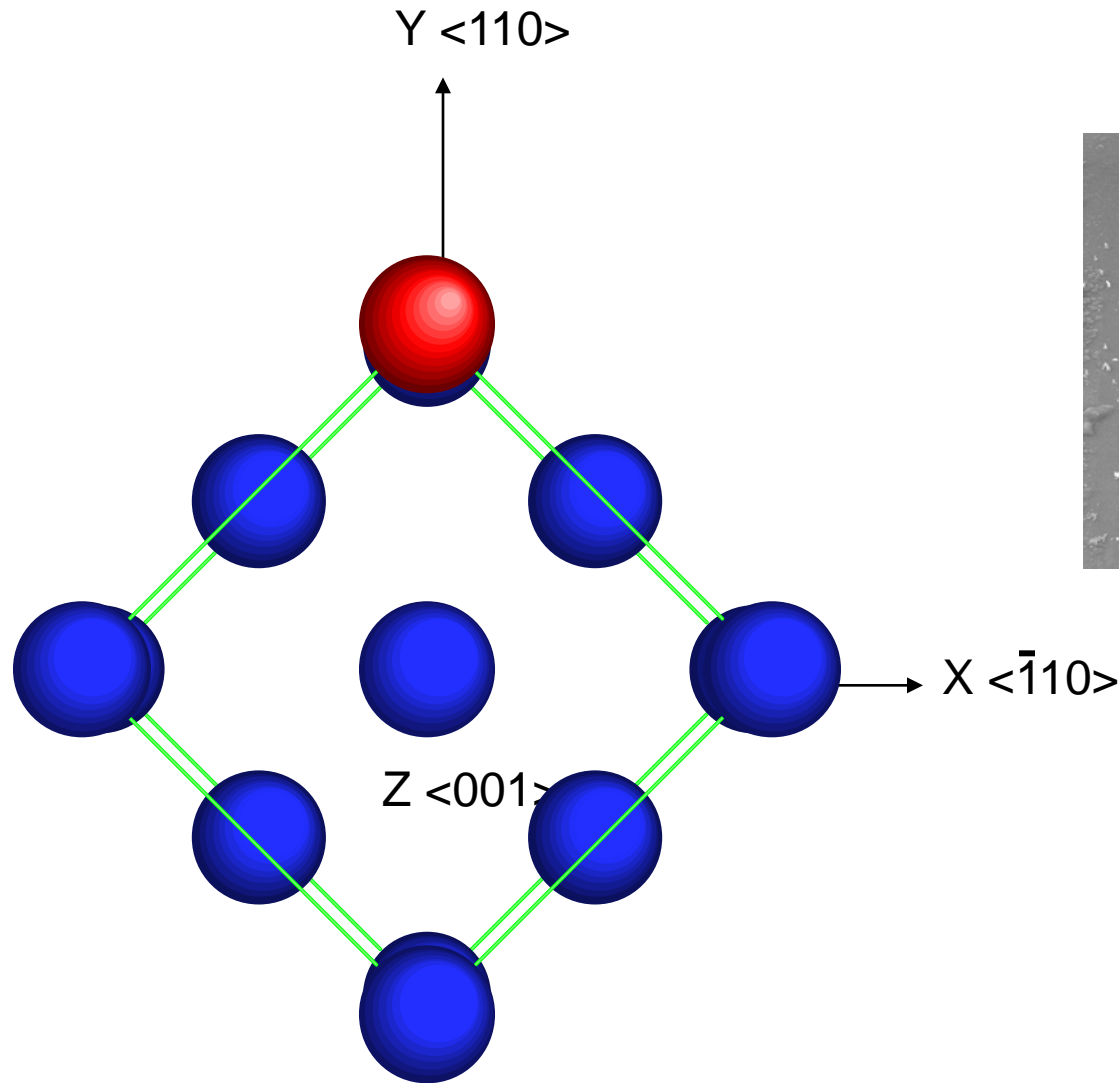
(100 grams for 200 Cycles)



101

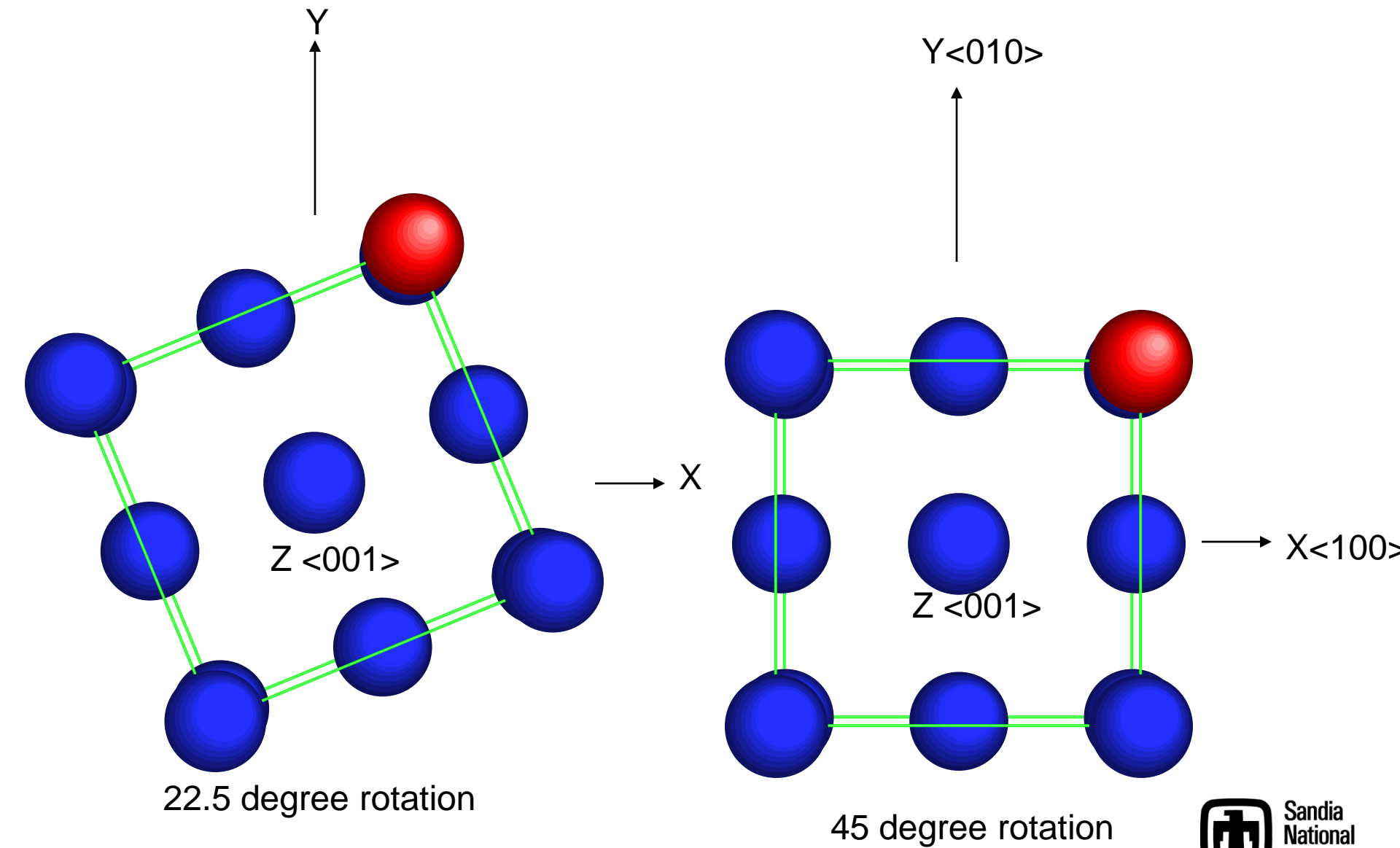


Schematic illustration of grain rotation. 1



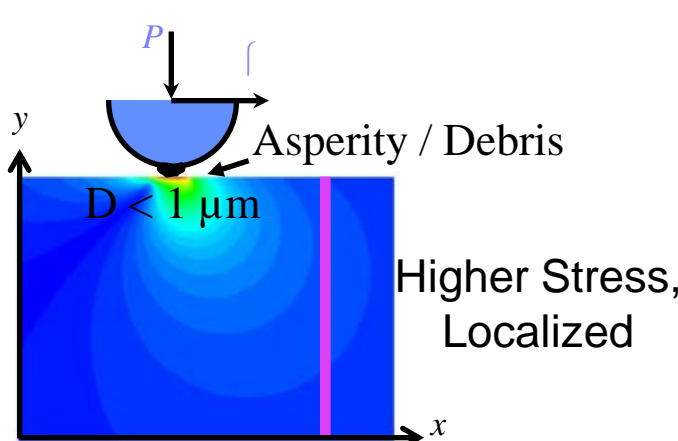
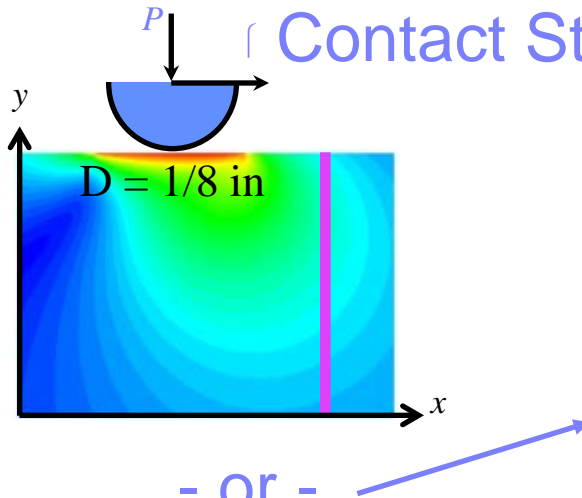


Schematic illustration of grain rotation. 2



Contact Mechanics and Crystal Plasticity

Frictional Elastic Contact Stresses³



Mechanical State

Material Properties

Deformation Model^{1,2}

$$\tau_{rss} = \frac{1}{2} \sigma : (\mathbf{d} \otimes \mathbf{n} + \mathbf{n} \otimes \mathbf{d})$$

$$\dot{\gamma} = \dot{\gamma}_o \left(\frac{\tau_{rss}}{\tau_{crss}} \right)^m$$

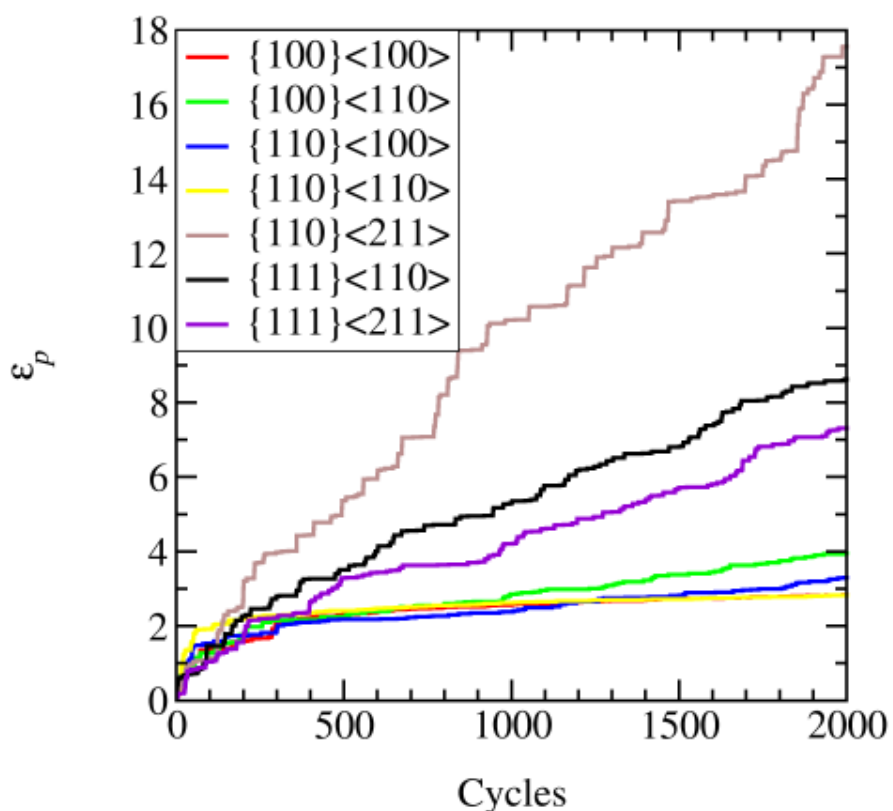
$$\dot{\mathbf{D}}_p = \frac{\dot{\gamma}}{2} (\mathbf{d} \otimes \mathbf{n} + \mathbf{n} \otimes \mathbf{d})$$

$$\Delta\epsilon_p = \Delta t \sqrt{\frac{2}{3} (\dot{\mathbf{D}}_p : \dot{\mathbf{D}}_p)}$$

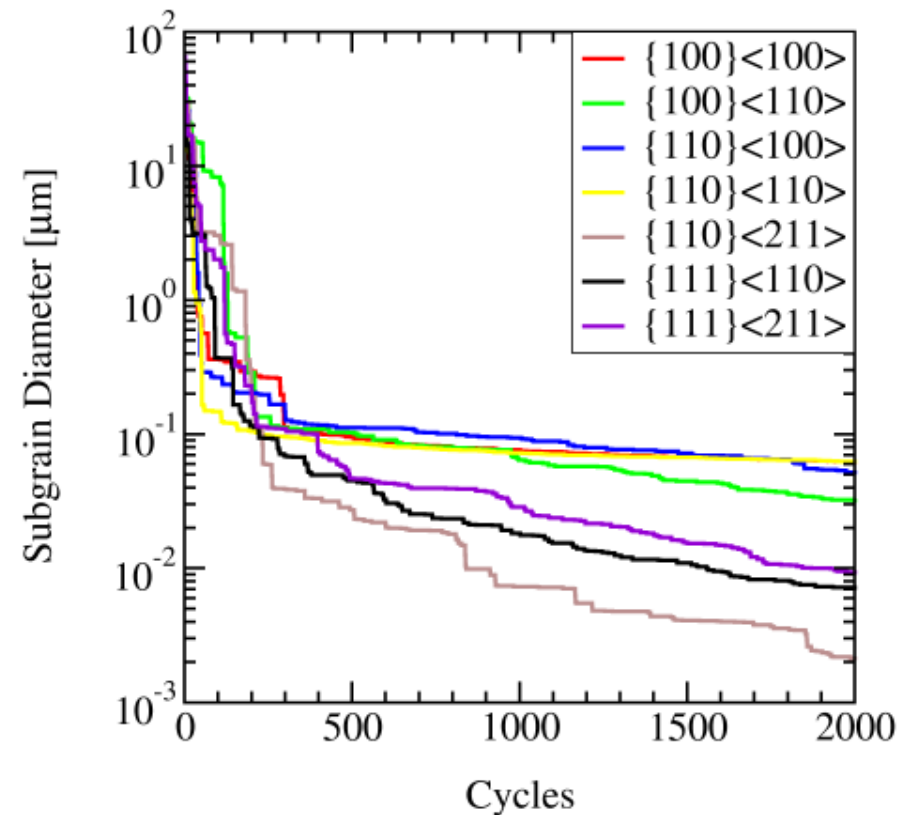
$$\tau_{crss} = \tau_o + A \left[1 - \exp \left(-\frac{n}{A} \epsilon_p \right) \right]$$

1. R.J. Asaro and J.R. Rice, "Strain Localization in Ductile Single Crystals," *J. Mech. Phys. Solids* **25** (1977) 309-38.
2. E. Voce, "The Relationship Between Stress and Strain for Homogeneous Deformation," *J. Inst. Metals* **74** (1948) 53.
3. D.A. Hills, D. Nowell, and A. Sackfield, *Mechanics of Elastic Contacts*, Oxford 1993.

Plastic Strain and Subgrain Formation (Model)



$$P = 1\text{N} \quad \mu = 0.8$$



$$d_{GNB} \approx \frac{0.724}{\epsilon^{1.12}} \text{ } \mu\text{m (for Al)}^1$$

1. A. Godfrey and D.A. Hughes, "Scaling of the Spacing of Deformation Induced Dislocation Boundaries," *Acta Mater.* **48** (2000) 1897.



Model: Qualitative Validation

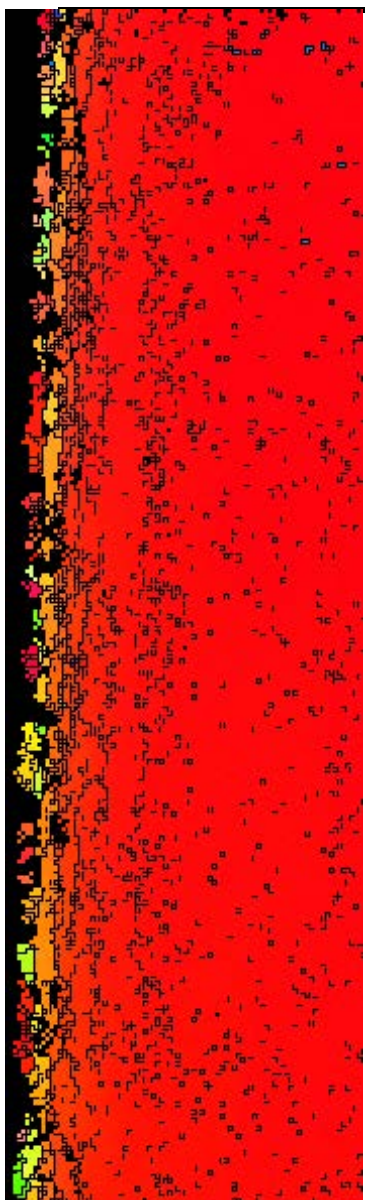
Increasing
Plastic Strain



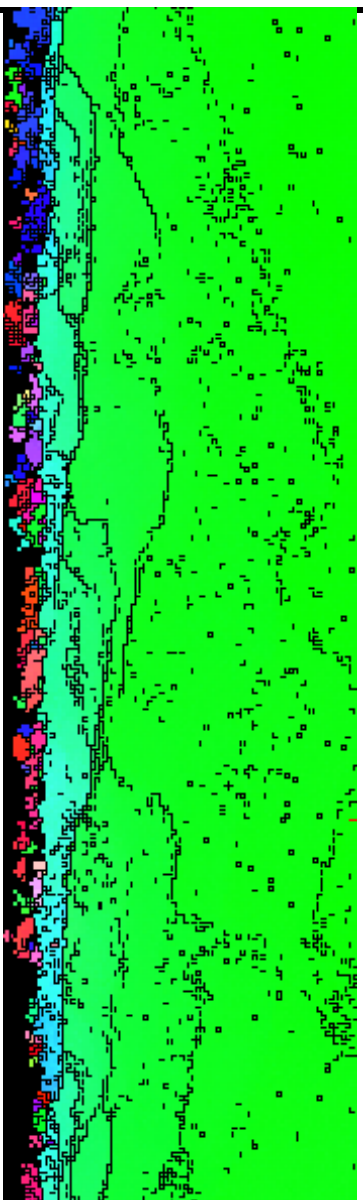
<u>Experimental Measurements</u>	<u>Model</u>
$\{100\}<100>$	$\{110\}<110>$
$\{110\}<100>$	$\{100\}<100>$
$\{110\}<110>$	$\{110\}<100>$
$\{100\}<110>$	$\{100\}<110>$
$\{111\}<110>$	$\{111\}<211>$
$\{111\}<211>$	$\{111\}<110>$
$\{110\}<211>$	$\{110\}<211>$

EBSD inverse pole figure maps of wear scars

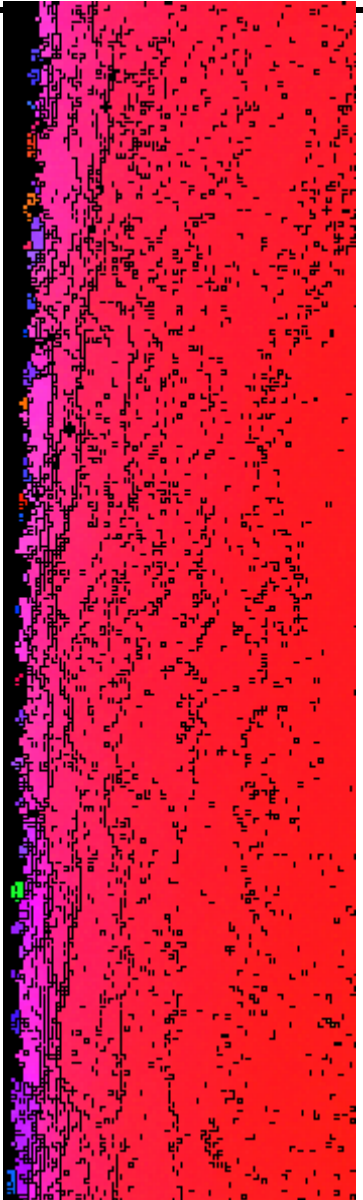
$<100>(001)$



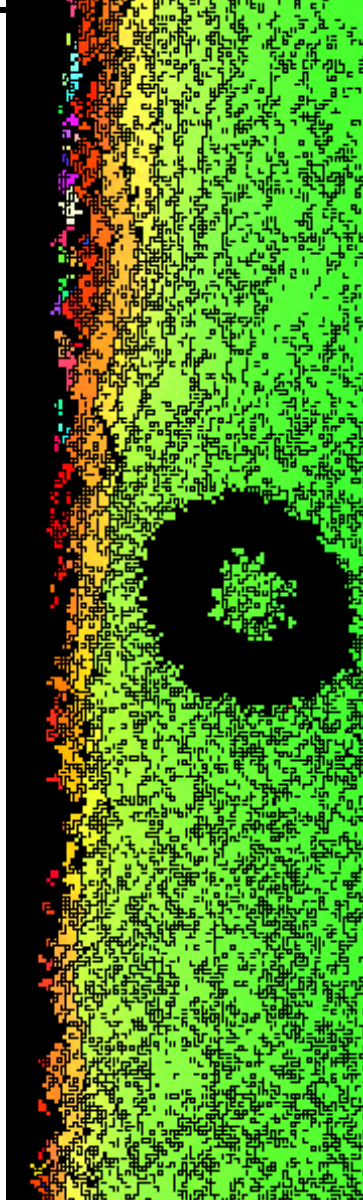
$<110>(001)$



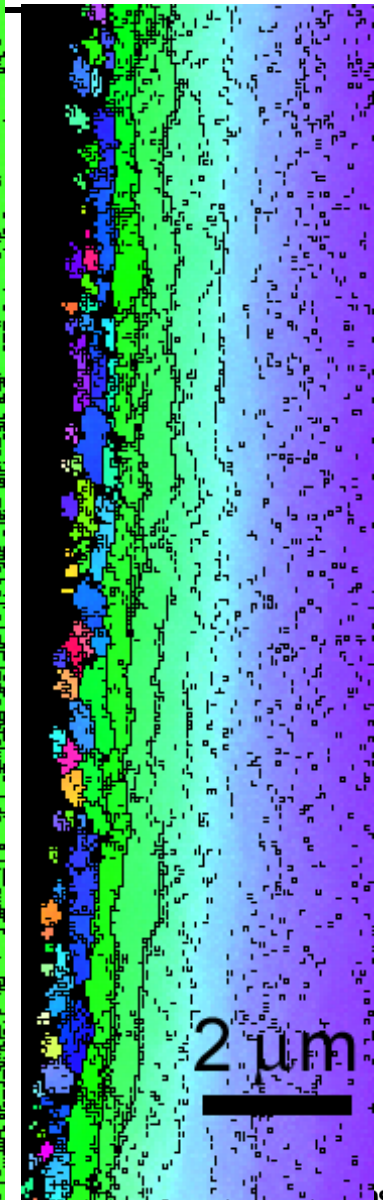
$<100>(011)$



$<110>(011)$



$<211>(011)$

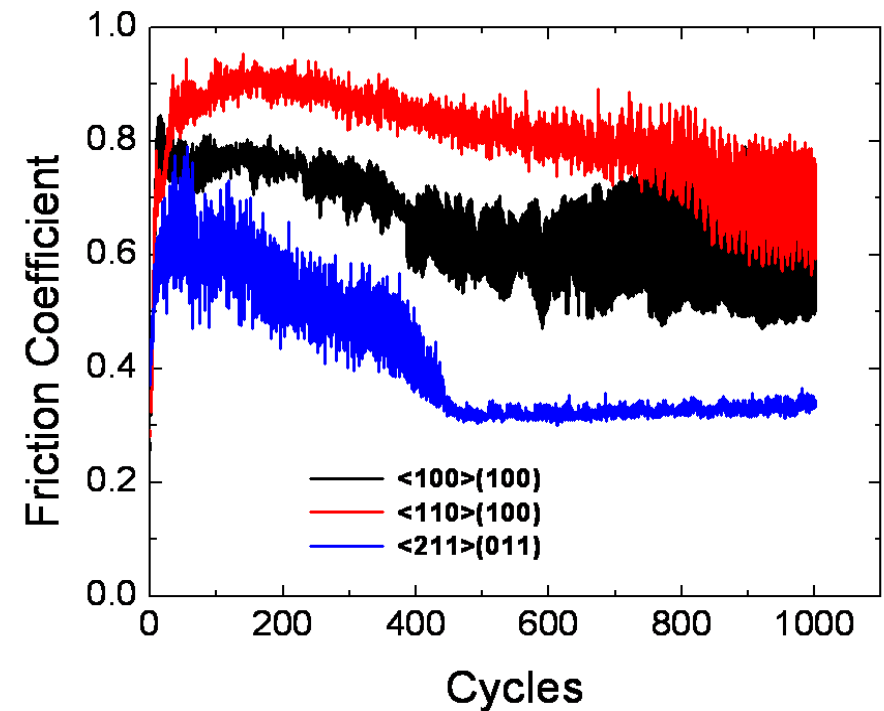
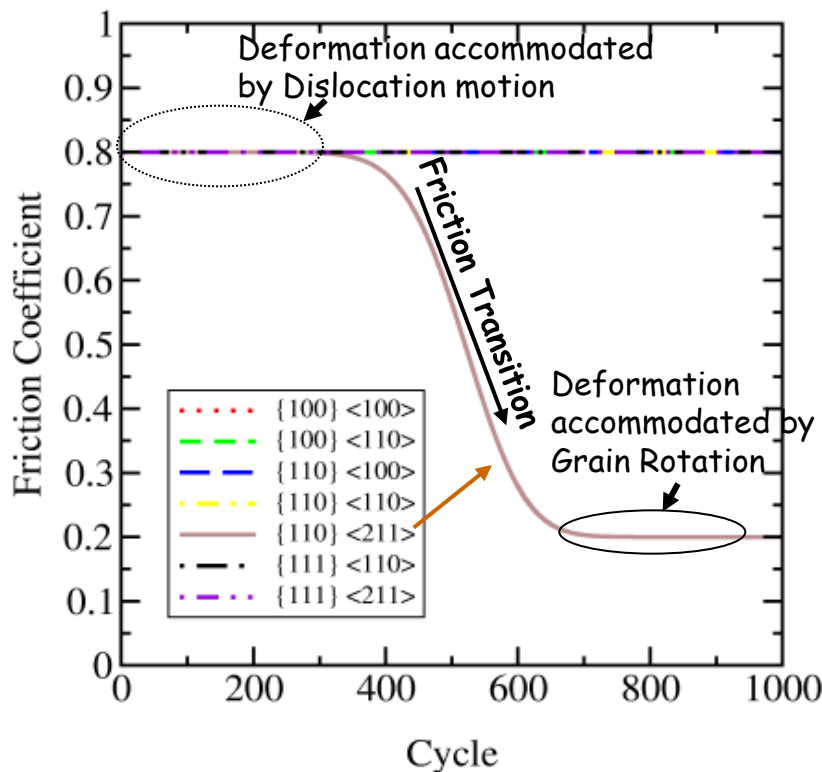


2 μm

Laboratories

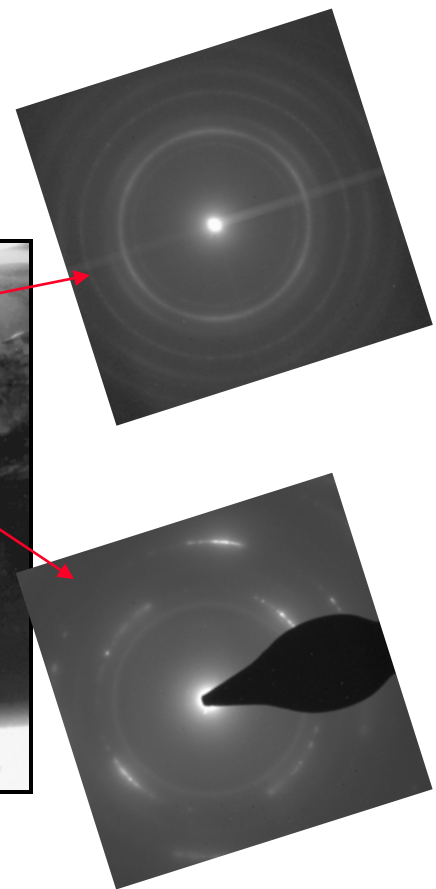
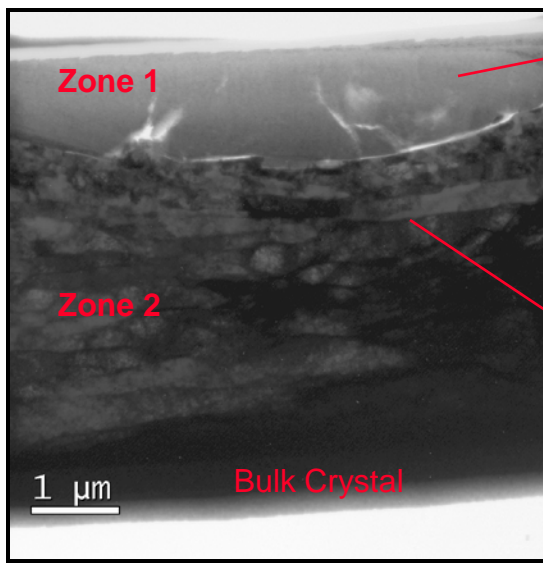
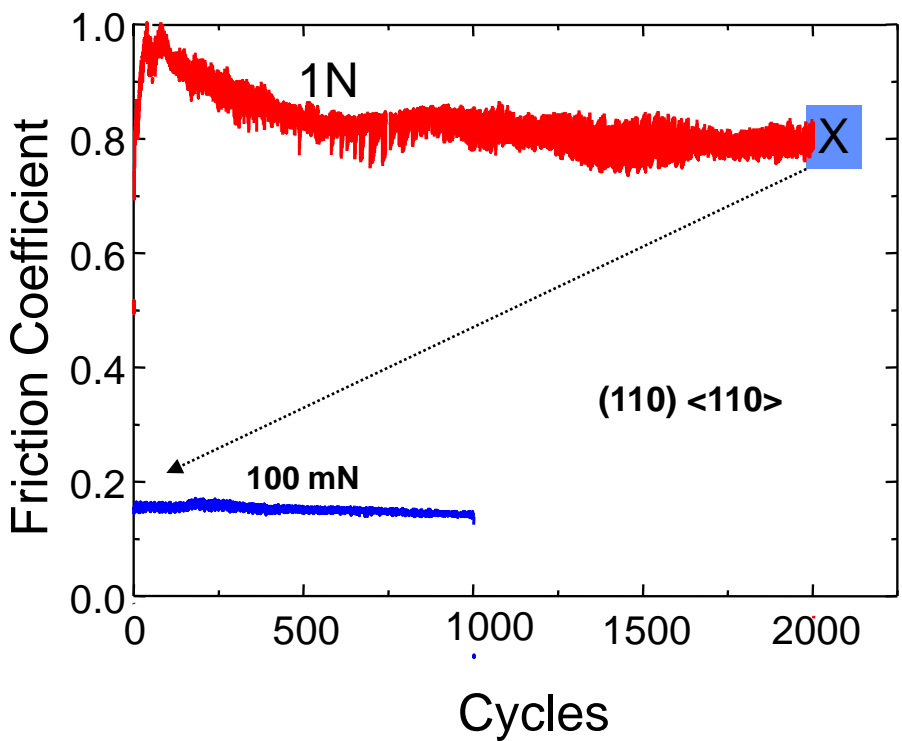
Grain Boundary Sliding Model

$$\boxed{\dot{\gamma}_{sp}} = \tau \frac{160\Omega}{kT} \frac{1}{d^2} \left(1 + \frac{\pi\delta}{d} \frac{D_{gb}}{D_{bk}} \right) D_{bk} \quad \longrightarrow \quad \mu = 0.2 + 0.6 \exp \left[-2 \left(\frac{\varepsilon_{gb}}{\varepsilon_p} \right)^2 \right]$$



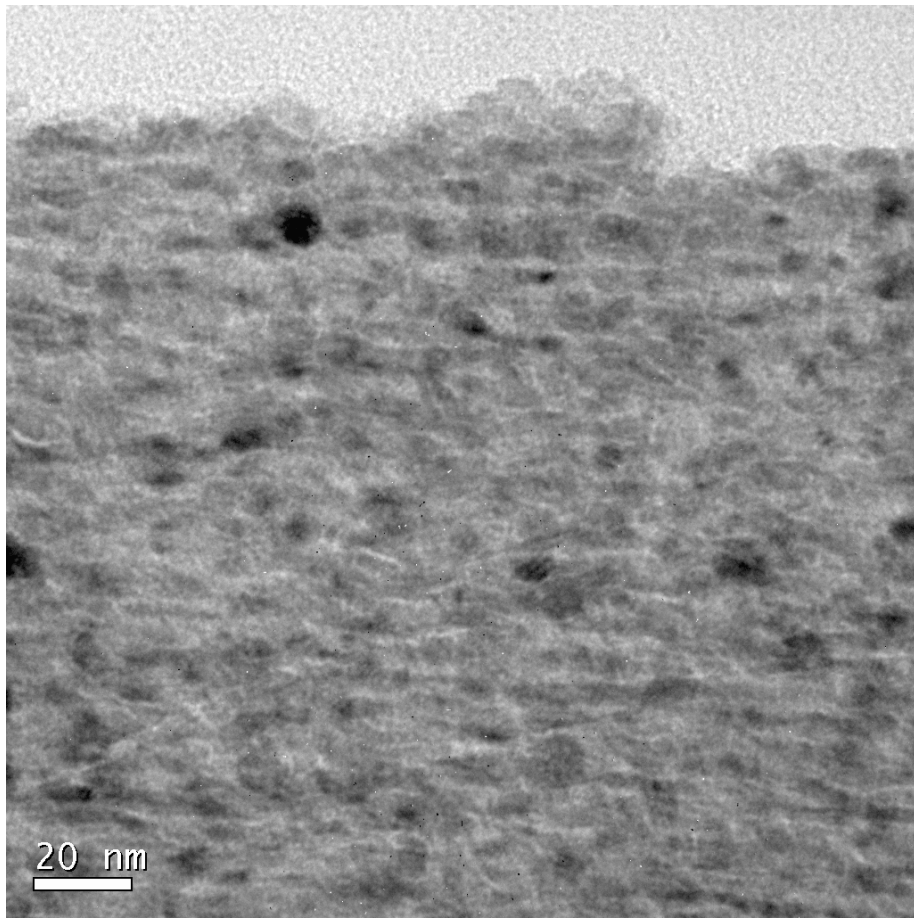


Higher normal loads (1N) produced unique substructures with interesting friction behavior

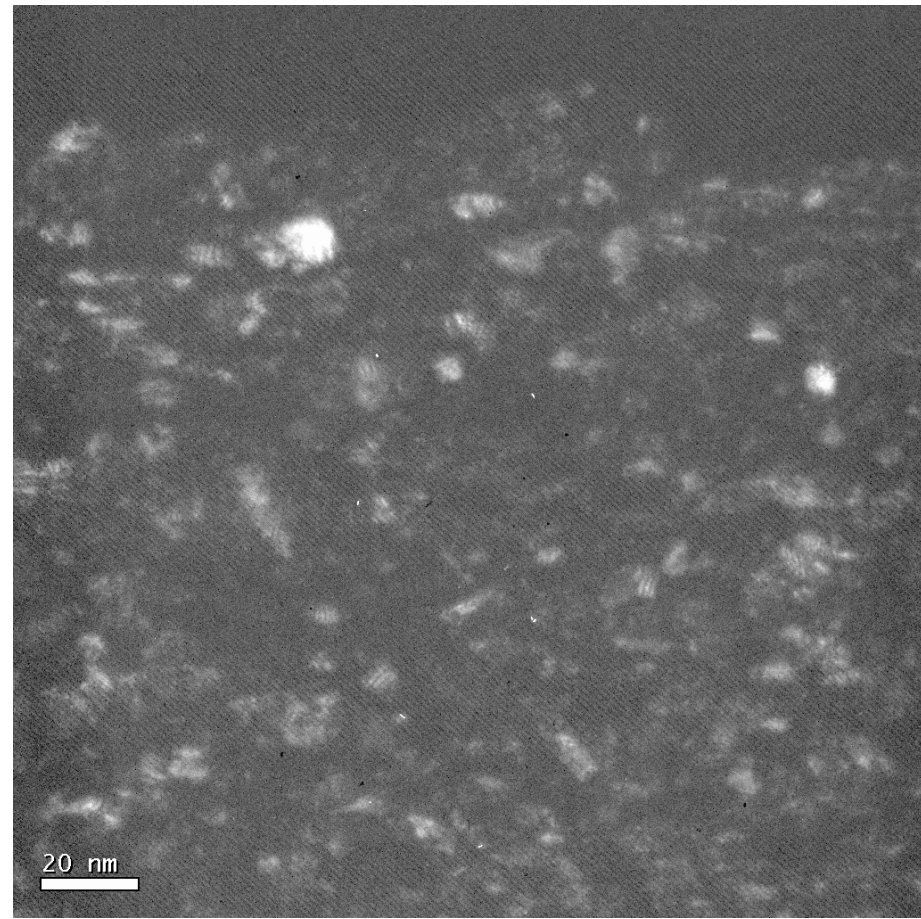




High resolution images of Zone 1



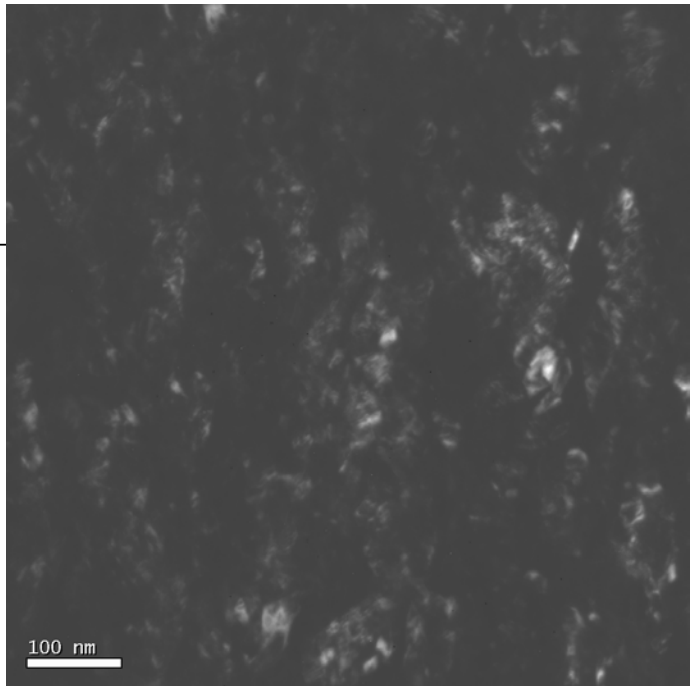
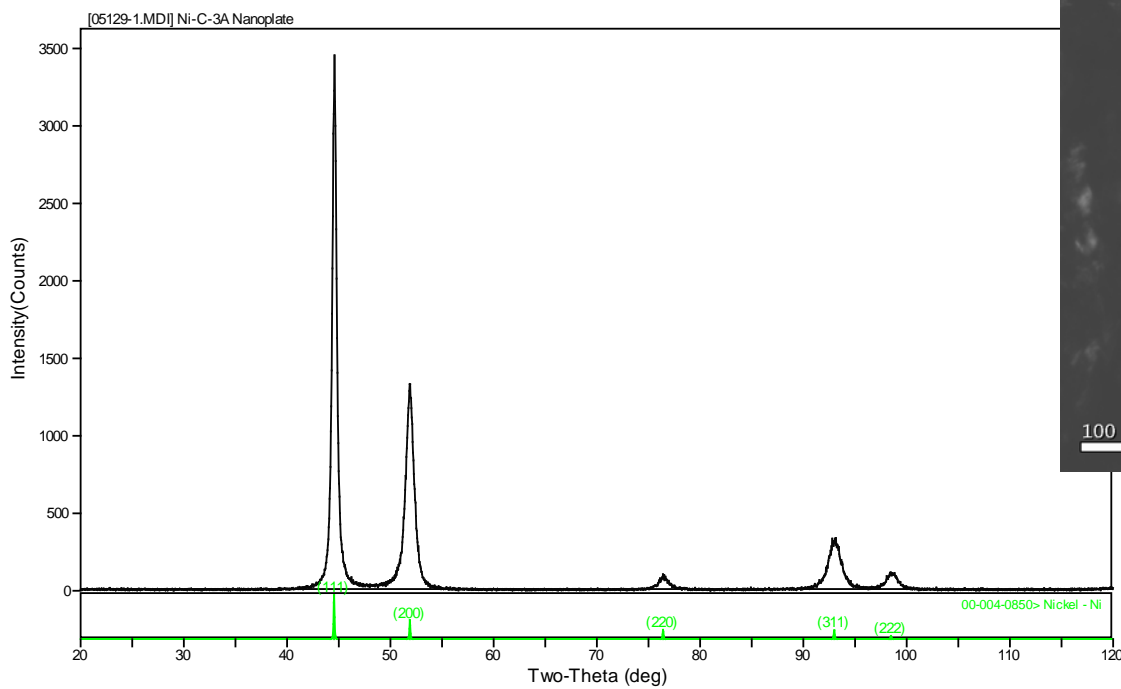
Bright-field TEM image



Dark-field TEM image



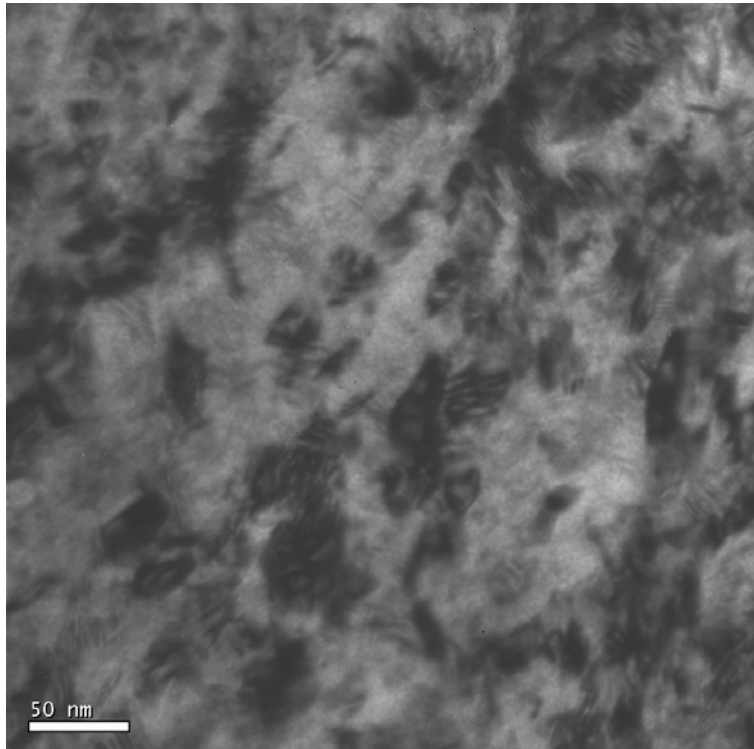
Part II: Application to Nanocrystalline Thin Films



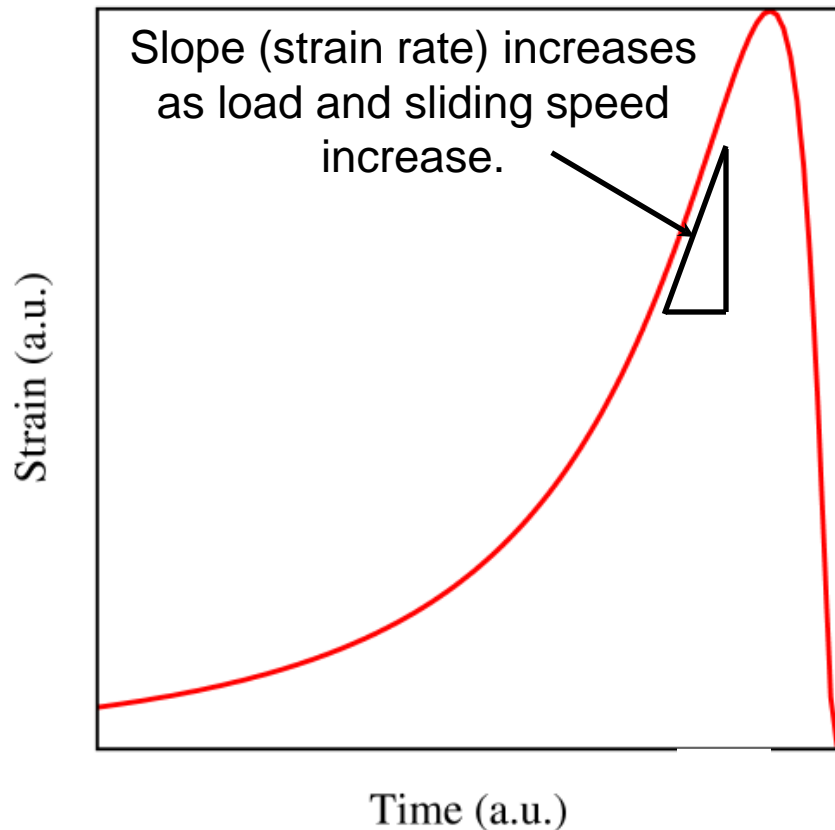


Nanocrystalline Ni Film: Strain Rate Effects

Load and sliding speed dictate subsurface strain rate

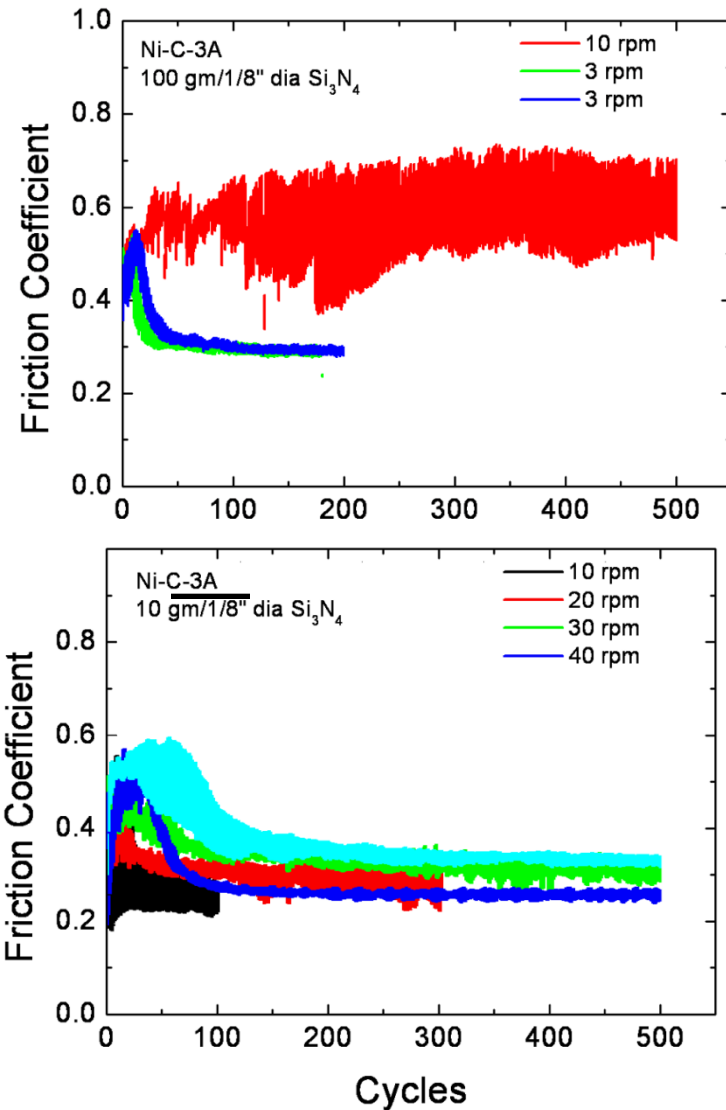


Bright-field TEM image

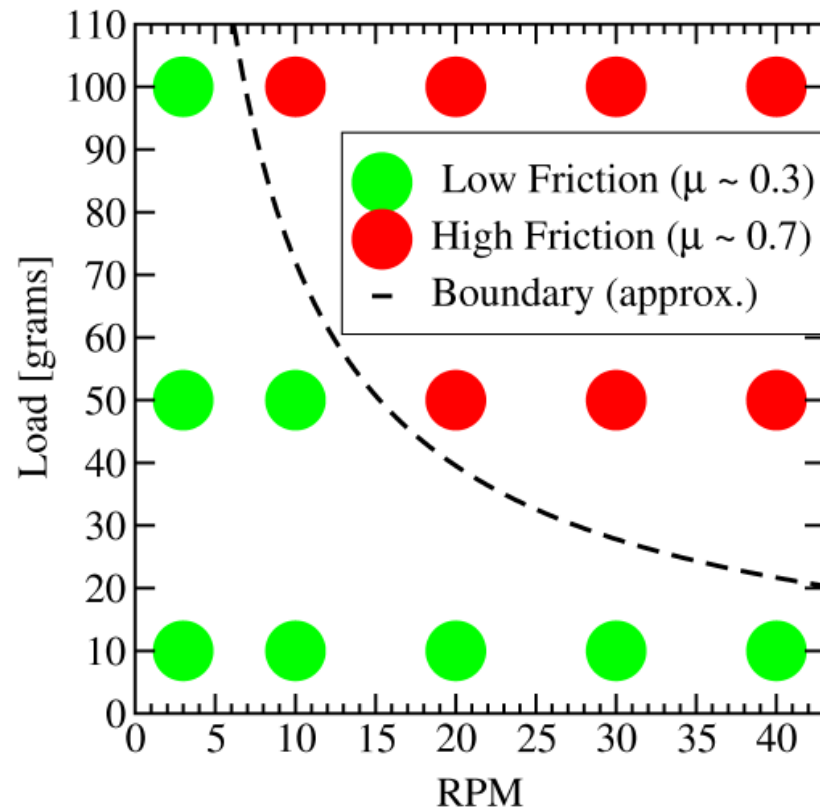


Schematic of the strain history experienced by the material below the worn surface.

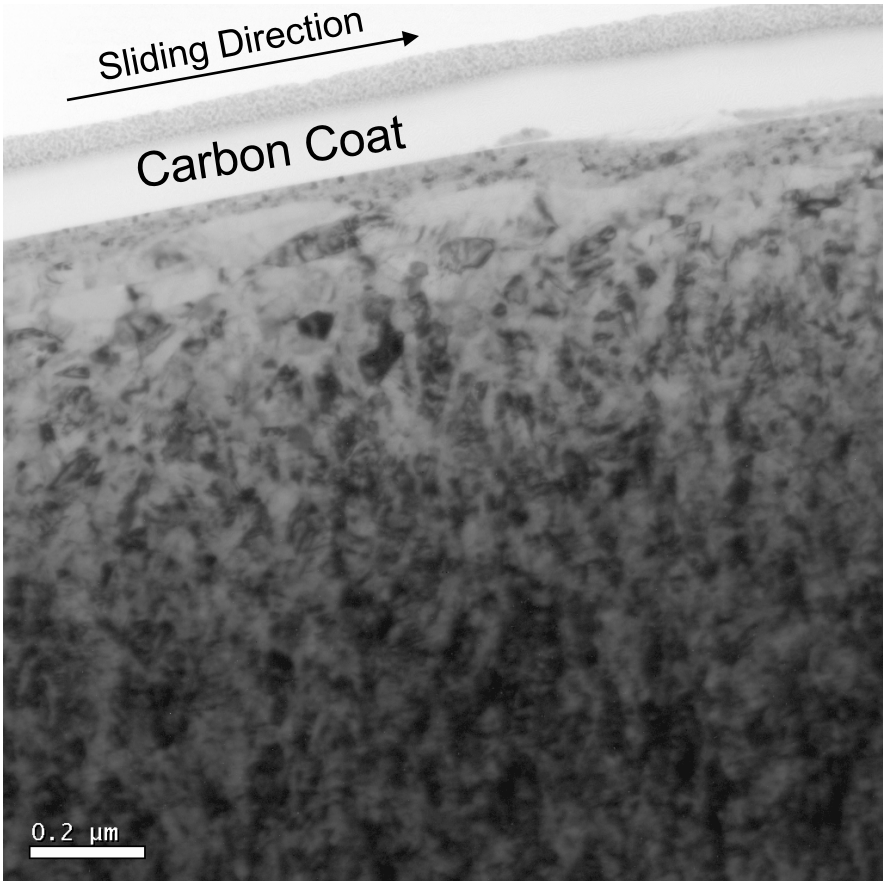
Nanocrystalline Ni: Strain Rate Effects on Friction



Transition to low friction
shows a clear dependence
on strain rate.

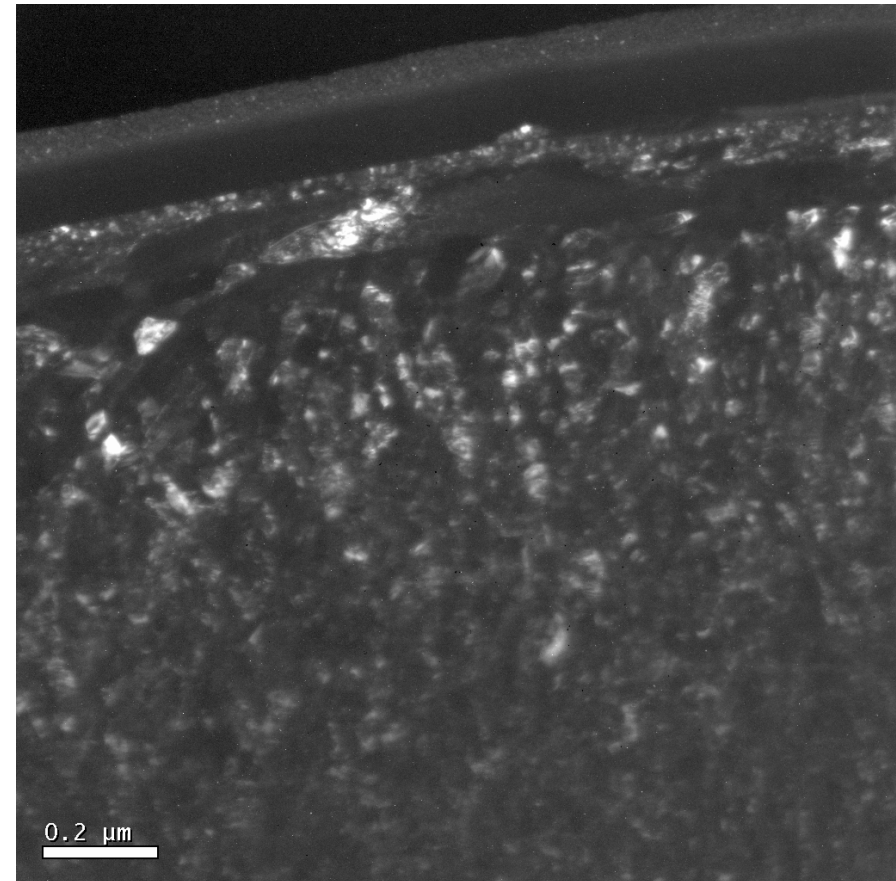


Transmission Electron Microscopy of Subsurfaces: Low Friction Case



BF-TEM

Sample preparation: FIB microscopy with low KeV cleaning
Low magnification micrographs



DF-TEM

Ni-3C-A1 #1 051202D Track 19, 10g, 20rpm, 600cycles

Higher Magnification Micrograph

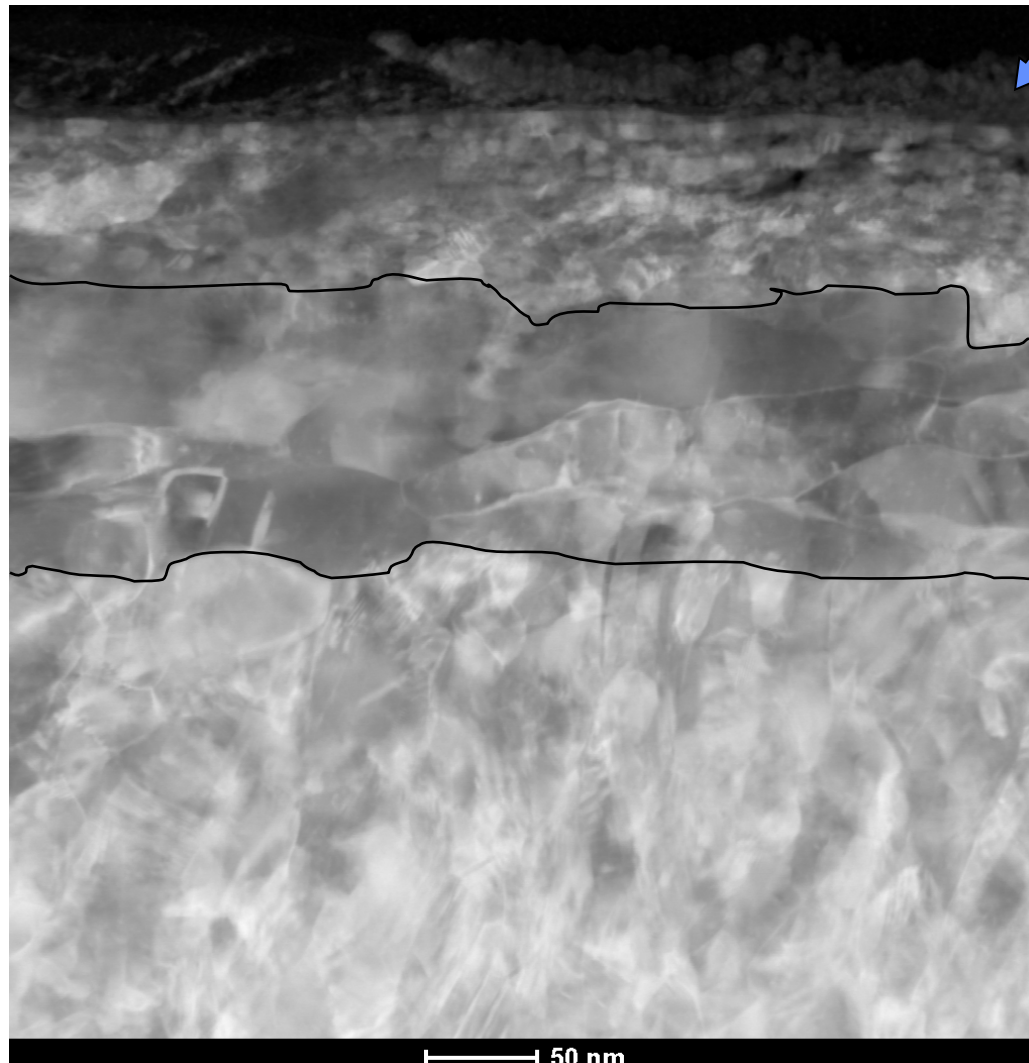
Zone 1
Ultra Nanocrystalline

Zone 2
Grain Growth +
Texture

Zone 3
Bulk

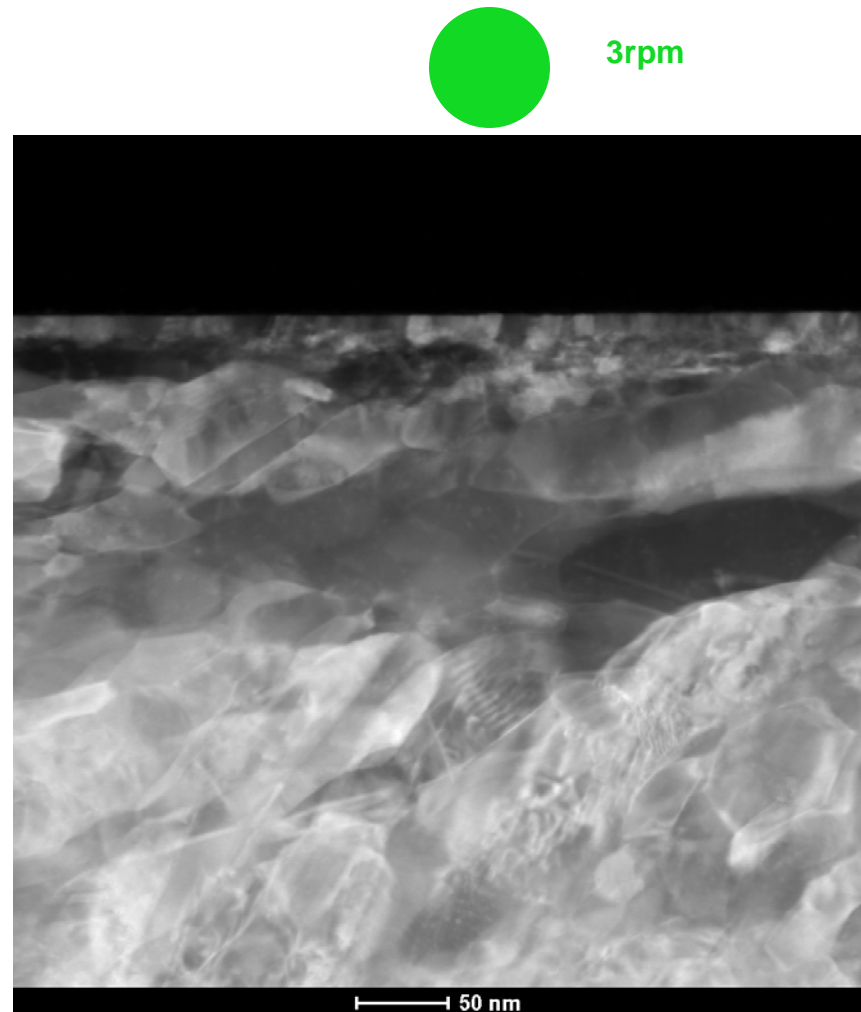
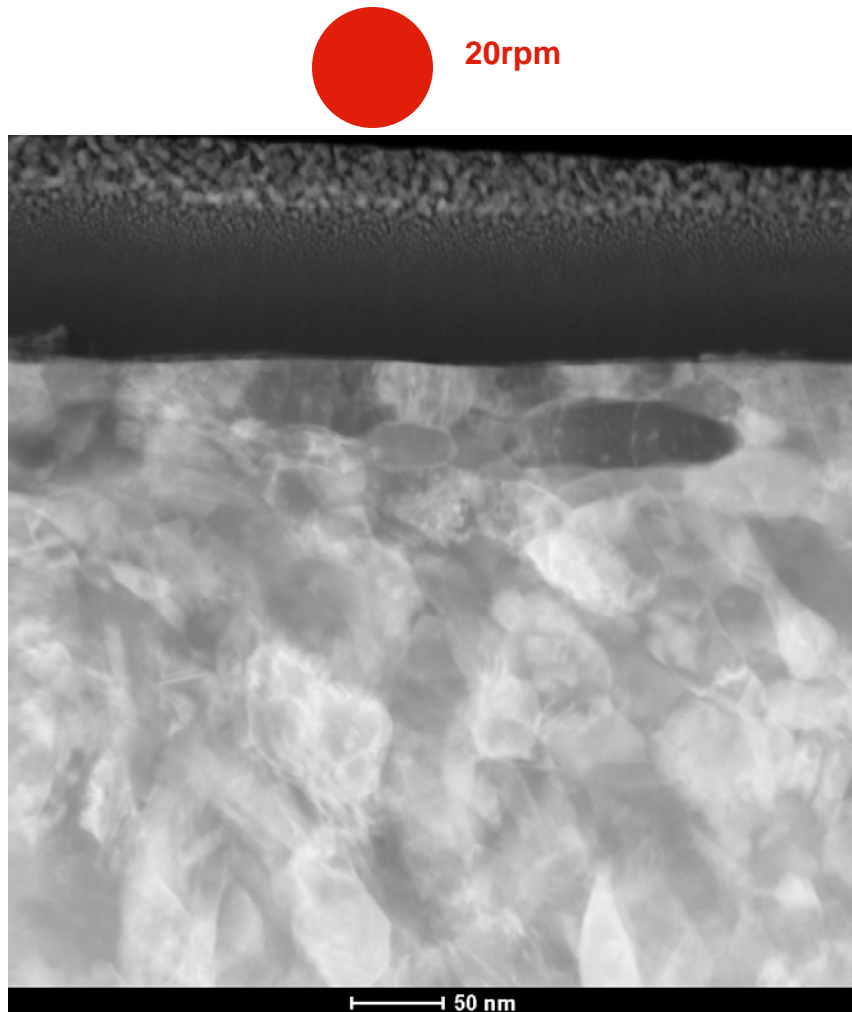
Annular DF Image

Ni-3C-A1 #1 051202D Track 19, 10g, 20rpm, 600cycles





Comparison of Subsurfaces: High Friction (Red) and Low friction (Green)



Annular DF STEM Images



Concluding Remarks

- Friction-induced deformation is related to crystallography
- Friction-induced deformation can generate nanostructures with unique friction characteristics
- Grain boundary sliding appears to be a viable deformation mechanism, and perhaps a route to mitigate metallic friction
- But the critical issues are: (a) friction-induced grain growth, and (b) stability of ultrananocrystalline zones.



Acknowledgements

Sandia National Laboratories is a multi-program laboratory managed and operated by Sandia Corporation, a wholly owned subsidiary of Lockheed Martin Corporation, for the U.S. Department of Energy's National Nuclear Security Administration under contract DE-AC04-94AL85000.

Rand Garfield for friction measurements

Supplementary Slides

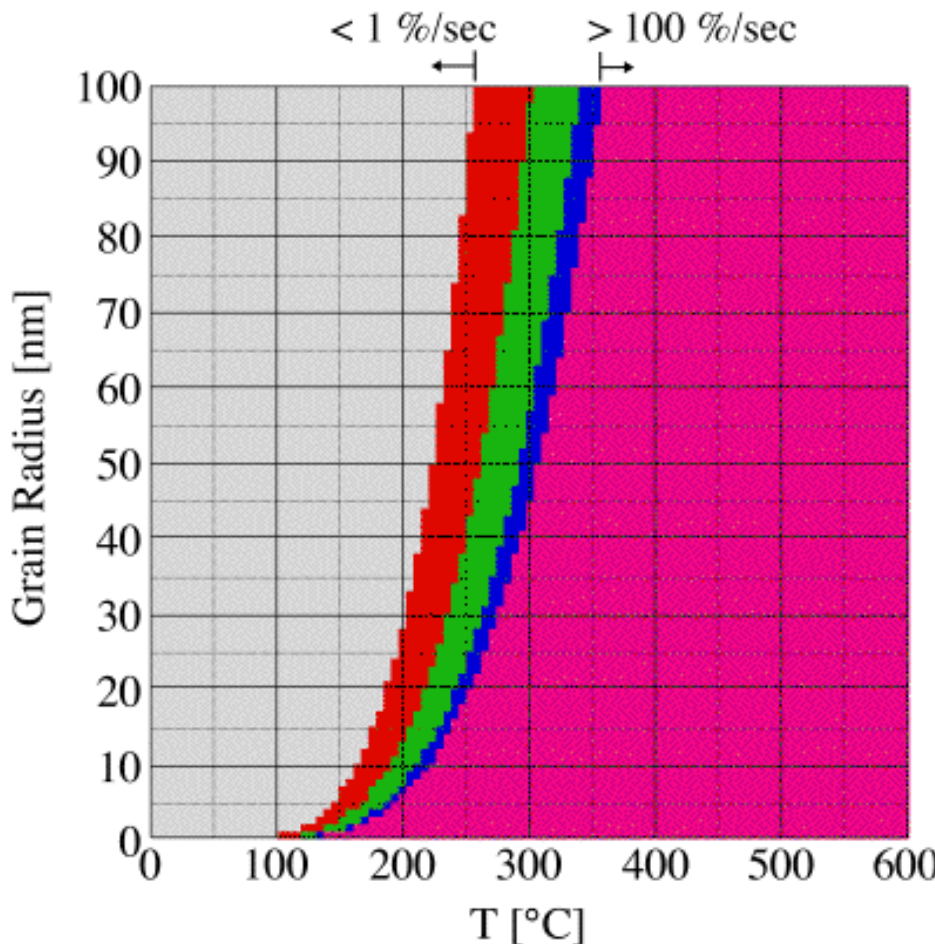


Raj and Ashby suggest a dependence of the grain-boundary-accommodated shear on the inverse of the cube of the grain size. Thus, very small grains might be expected to slide or rotate, even at room temperature. If we postulate an exponential dependence of the friction coefficient on the ratio between grain boundary and dislocation straining, and we bound the functional form according to the experimentally observed friction limits, i.e. 0.2 and 0.6, then we qualitatively reproduce the friction behavior observed experimentally.



The material model for dislocation plasticity is based on a reduced form of continuum crystal plasticity. The stress tensor, sigma, is projected, i.e. resolved, onto each slip system. The resulting resolved shear stress, tau_rss, relative to the critical value, tau_crss, determines the rate of dislocation slip, gamma_dot. This, in turn, is projected onto the slip geometry to produce the plastic strain rate tensor. An invariant of this tensor, integrated in time, is used to calculate the plastic strain increment, and the total plastic strain is used to update the critical resolved shear stress for the next cycle.

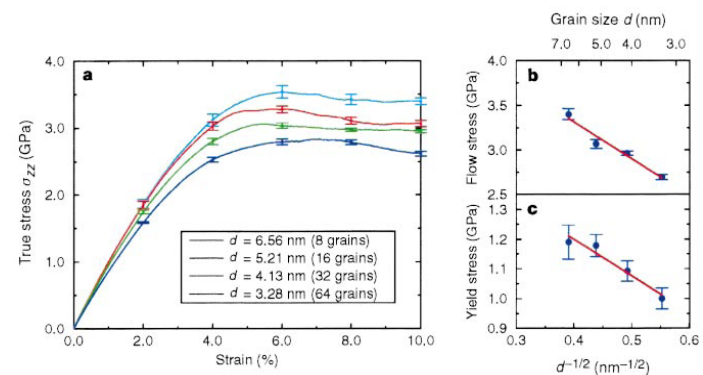
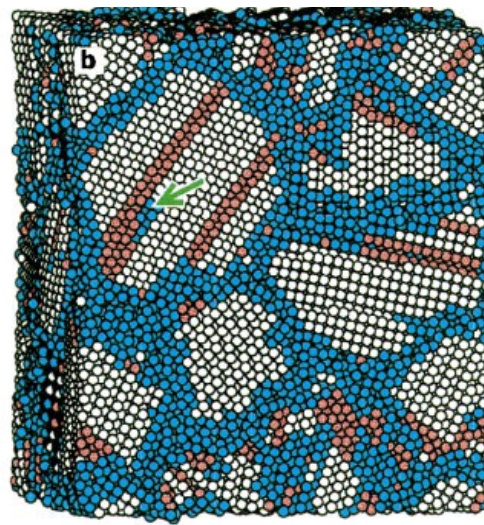
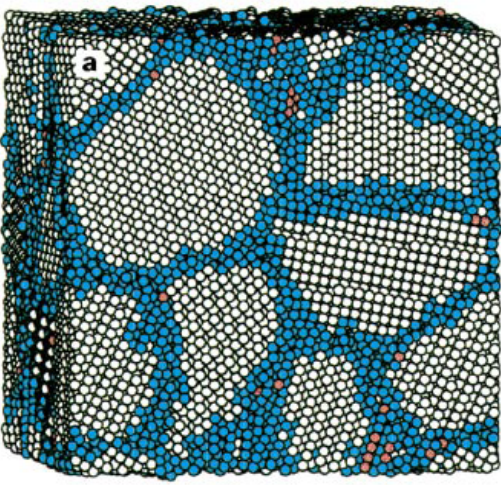
Grain Boundary Sliding and Diffusional Creep



Contour Map of Shear Strain Rates
From Grain Boundary Sliding¹

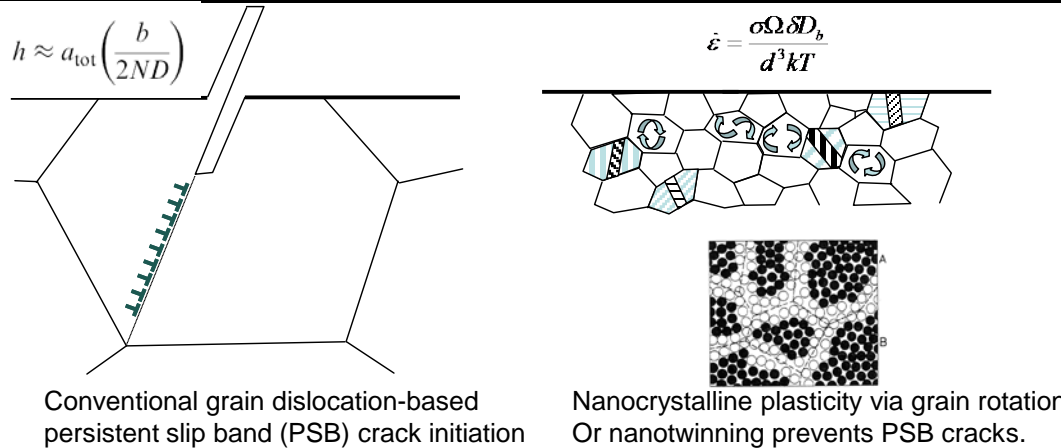
$$\dot{\gamma} = \tau \frac{160\Omega}{kT} \frac{1}{d^2} \left(1 + \frac{\pi\delta}{d} \frac{D_{gb}}{D_{bk}} \right) D_{bk}$$

R. Raj and M.F. Ashby, "Grain Boundary Sliding and Diffusional Creep," *Met. Trans.* **2** (1971) 1113.

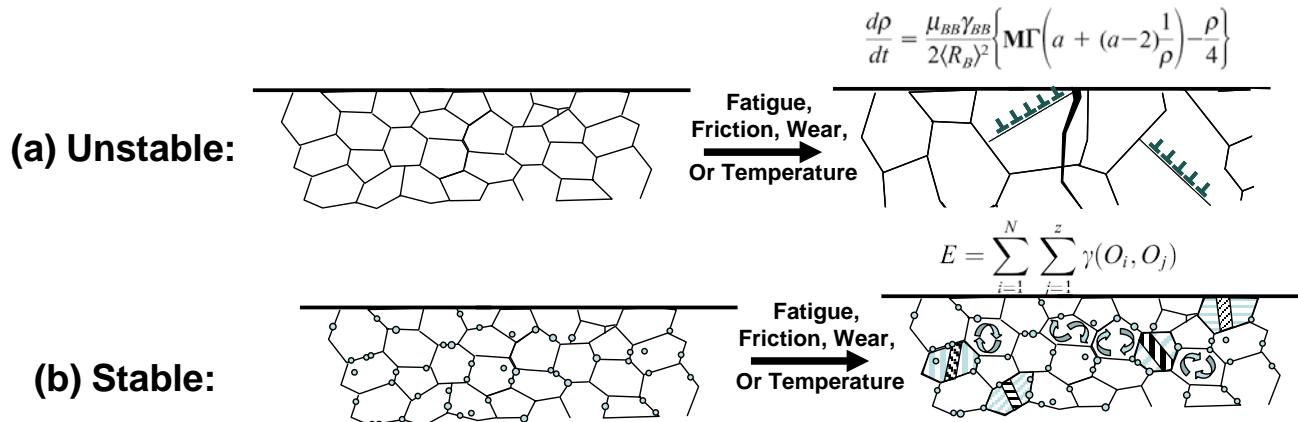


TWO KEY ENABLING MECHANISMS

1. Suppress length-scale for dislocation-mediated plastic damage modes



2. Stabilize beneficial nanodomains against thermal or mechanical coarsening



New Science:

- (a) Exploit length-scale transition from dislocations to alternative nanoscale mechanisms (twinning, grain rotation).
- (b) A nanoscale grain-growth model with incorporation of Zener pinning and solute drag to predict nanodomain stability.
- (c) Grain-size effects predicted by MD-informed grain-boundary interactions in a dislocation dynamics framework
- (d) Understand failure mechanisms (crack initiation, frictional accommodation) in dislocation-starved scenarios.

